

# CHALMERS



## A control system and power electronic for an electric powertrain implemented on a go-kart

*Master of Science Thesis in the Programme Integrated Electronic System Design*

Fredrik Lönnblad  
Andreas Öhlund

Chalmers University of Technology  
University of Gothenburg  
Department of Computer Science and Engineering  
Göteborg, Sweden, December 2012

The Author grants to Chalmers University of Technology and University of Gothenburg the non-exclusive right to publish the Work electronically and in a non-commercial purpose make it accessible on the Internet.

The Author warrants that he/she is the author to the Work, and warrants that the Work does not contain text, pictures or other material that violates copyright law.

The Author shall, when transferring the rights of the Work to a third party (for example a publisher or a company), acknowledge the third party about this agreement. If the Author has signed a copyright agreement with a third party regarding the Work, the Author warrants hereby that he/she has obtained any necessary permission from this third party to let Chalmers University of Technology and University of Gothenburg store the Work electronically and make it accessible on the Internet.

A control system and power electronic for an electric powertrain implemented on a go-kart

Fredrik Lönnblad  
Andreas Öhlund

© Fredrik Lönnblad, December 2012.

© Andreas Öhlund, December 2012.

Examiner: Lars Svensson

Chalmers University of Technology  
University of Gothenburg  
Department of Computer Science and Engineering  
SE-412 96 Göteborg  
Sweden  
Telephone + 46 (0)31-772 1000

Department of Computer Science and Engineering  
Göteborg, Sweden December 2012

### **Acknowledgements**

Thanks QRTECH AB for having us and all the help with this project.

## **Abstract**

This report describes the master thesis project where a 3-phase AC-inverter is designed with software to space vector modulate the output currents. The report outlines a brief background to the project and then goes on to describe the demands that the inverter must fulfill. The controlling software is described both in general and the application specifics are treated. The hardware solution is described and major component choices are discussed. The complete working inverter was successfully implemented on a go-kart, and the testing verifies that the functionality of the inverter is according to the specifications. The inverter was not fully tested to the upper limits of 72V and 300V peak current due to lack of testing equipment, though the results are promising for the inverter to be able to handle this.

# Contents

<b>1</b>	<b>Introduction</b>	<b>1</b>
1.1	Background . . . . .	1
1.2	Goal . . . . .	1
1.3	Specification of Requirements . . . . .	1
1.4	Restrictions . . . . .	2
1.5	Resources . . . . .	3
1.6	Course of action . . . . .	3
<b>2</b>	<b>Electric Powertrain</b>	<b>4</b>
2.1	Power Electronic Converters . . . . .	4
2.1.1	Space Vector Modulation . . . . .	5
2.2	Permanent Magnet Synchronous Motor (PMSM) . . . . .	6
<b>3</b>	<b>System fault-tolerance and robustness</b>	<b>8</b>
3.1	Analysis . . . . .	8
3.2	Solutions . . . . .	8
<b>4</b>	<b>System overview</b>	<b>11</b>
<b>5</b>	<b>Electronic Control Unit "ECU"</b>	<b>12</b>
5.1	Torque Control Loop . . . . .	12
5.1.1	Current Measurement . . . . .	12
5.1.2	Electrical Angle . . . . .	13
5.1.3	Mechanical RPM . . . . .	13
5.1.4	Clarke transformation . . . . .	13
5.1.5	Park's transformation . . . . .	14
5.1.6	$d$ - and $q$ -torque regulators . . . . .	15
5.1.7	PID . . . . .	16
5.1.8	Sector Calculations . . . . .	18
5.2	Fan Controller . . . . .	19
<b>6</b>	<b>DSP and software specific to this project</b>	<b>20</b>
6.1	DSP - TMS320F28335 . . . . .	20
6.2	Electric Angle from pulsetrain . . . . .	21
6.3	Torque Reference . . . . .	21
6.3.1	Potentiometer . . . . .	21
6.4	Temperature measurement . . . . .	22
<b>7</b>	<b>Hardware</b>	<b>24</b>
7.1	Hardware overview . . . . .	24
7.2	Description of the system blocks . . . . .	25
7.2.1	CAN & peripherals . . . . .	25
7.2.2	Current sensors, resolver and miscellaneous sensors . . . . .	25

7.2.3	Gate drivers . . . . .	26
7.2.4	Isolated power . . . . .	27
7.2.5	Half brigdes . . . . .	27
7.3	Component choices . . . . .	28
7.3.1	Traco power modules . . . . .	28
7.3.2	MOSFET transistors . . . . .	28
7.3.3	Reverse recovery capacitors . . . . .	30
7.3.4	Snubber circuit . . . . .	31
7.4	PCB Layout . . . . .	32
7.4.1	Power PCB . . . . .	32
7.4.2	Controller PCB . . . . .	33
<b>8</b>	<b>Building and intregrating a powertrain on a Go-Kart</b>	<b>36</b>
8.1	Cooling . . . . .	36
8.1.1	Heat sink . . . . .	37
8.1.2	Fan . . . . .	37
8.2	Encasing . . . . .	39
8.3	Batteries / Charging . . . . .	39
8.4	Resolver . . . . .	39
8.4.1	Resolver-to-Digital Converter . . . . .	41
8.4.2	Resolver Mount . . . . .	41
8.5	Drive line . . . . .	43
8.6	Engine mount . . . . .	44
8.7	Inverter mount . . . . .	44
8.8	Front panel . . . . .	45
<b>9</b>	<b>Verification and testing</b>	<b>47</b>
9.1	Software . . . . .	47
9.1.1	Verification of Current Measurement Calibration . . . . .	47
9.1.2	Verification of Current Measurement . . . . .	47
9.1.3	Verification of Accelerator reference . . . . .	47
9.1.4	Verification of Fan control and temp measurement . . . . .	48
9.1.5	Verification of interrupt duty cycle . . . . .	48
9.1.6	Verification of switching ADC-channels . . . . .	48
9.1.7	Verification of the Driver Disable . . . . .	48
9.1.8	Verification of the Speed Measurement . . . . .	49
9.2	Hardware . . . . .	49
<b>10</b>	<b>Result</b>	<b>52</b>
<b>11</b>	<b>Discussion</b>	<b>53</b>
<b>12</b>	<b>Conclusion</b>	<b>57</b>
	<b>References</b>	<b>58</b>

A Control PCB schematics	I
B Power PCB schematics	XVII

## List of Abbreviations

AC	Alternating Current
ADC	Analog to Digital Converter
ATO	Angle Tracing Observer
BEV	Battery Electric Vehicle
CAN	Controller Area Network
DC	Direct current
DSP	Digital Signal Processor
ECU	Electric Control Unit
EMC	Electro Magnetic Compatibility
EMI	Electro Magnetic Interference
ESD	Electro Static Discharge
EV	Electric Vehicle
GND	Ground
GPIO	General Purpose Input Output
HEV	Hybrid Electric Vehicle
IC	Integrated Circuit
IGBT	Isolated Gate Bipolar Transistor
IR	Infra Red
JTAG	Joint Test Action Group
LED	Light Emitting Diode
LUT	Look-Up Table
Mbps	Mega bit per second
MOSFET	Metal Oxide Semiconductor Field Effect Transistor
MSPS	Mega Samples per Second
NTC	Negative Temperature Coefficient
PCB	Printed Circuit Board
PHEV	Plug-in Hybrid Electric Vehicle
PMSM	Permanent Magnet Synchronous Machine

PTC Positive Temperature Coefficient  
PWM Pulse Width Modulation  
QEP Quadrature Encoder Pulse  
R/D Resolver to Digital  
RMS Root Mean Square  
RPM Revolutions Per Minutes

# 1 Introduction

This report describes a proposed design and its implementation for an inverter and its control system in an electric powertrain. The report will also include sections on how this inverter was integrated in a real powertrain on a go-kart.

This introduction describes the motivations behind the project and how it was carried out.

## 1.1 Background

Presently, roughly every sixth human on earth has a car in general, summing up to a total of around a billion cars[1]. Looking at Sweden, around every second citizen own a passenger car[2], if this would have been the case globally, the total number of cars in the world would be roughly 4 billion in 2025[3]. However projections say that the number will be around 2 billion, largely a consequence of China's and India's growth, this is still a double to the current amount. Given that greenhouse gases are already causing problems with our climate, air-pollution is a major concern in our cities and that conflicts in unstable oil-rich nations is a current reality, realistic solutions need to be found[1].

With this in mind QRTECH seeks to expand its current product portfolio within power electronics and develops DC/DC-converters, inverters, on-board chargers and battery systems for the automotive industry.

## 1.2 Goal

The primary goal of this project is to redesign an existing inverter to fit a changed set of demands. Analysis and implementation of safety mechanisms is also a central part to guarantee robustness and fault-tolerance. Second to this is that the inverter is to be implemented with a complete drive line on an electric go-kart and make it drivable.

## 1.3 Specification of Requirements

This section describes a set of requirements that were developed out of discussions between the project group and QRTECH.

### Supply Voltage

The system shall be designed for a DC supply voltage between 40-70 volts.

### **3 phase current**

The system shall be designed for a 3 phase AC and be able to handle peaks up to 300A.

### **Torque control**

The system shall utilize a closed feedback-loop with a pair of torque-setpoints, current-measurement as feedback together with the rotor-angle of the PMSM.

### **Cooling**

The system shall have both an active (fan) and a passive (heat sink) cooling system to prevent the inverter from overheating and possibly sustaining damage.

### **Mechanical**

The system shall be implemented on a go-kart and therefore mechanical parts shall be designed and manufactured to enable this.

### **CAN**

The system shall have support for CAN-communication[4] to enable future development of communication and interactions with the inverter.

### **Safety aspects**

The system shall be designed with safety aspects in terms fault-tolerance and robustness in mind.

### **Angle measurement**

The system shall utilize resolver type sensor and a R/D (Resolver to Digital) Converter IC, prechosen by QRTECH, for the the angle feedback from the motor to the control loop.

## **1.4 Restrictions**

This section presents some parts that are outside the scope of this project and/or already a part of an older version of this system.

### **Motor**

The motor is a part of the old system and is therefore predetermined.

### **Regenerative breaking**

Software implementation of regenerative breaking is outside the scope of this project.

### **Chassi**

The go-kart chassis is a part of the old project and is therefore predetermined.

**Battery**

The batteries are a part of the old project and are therefore predetermined.

**DSP**

Since the DSP is prechosen by QRTECH, analysis will not be carried out.

**CAN**

Software implementation of CAN is outside the scope of this project.

## 1.5 Resources

In this section, a brief listing of the resources available for the project is presented.

**1600 man-hours**

A total of 1600 man-hours over 20 weeks, divided on a 2 man group are available.

**QRTECH AB**

QRTECH AB offered a lot of the resources to make this project possible. Among them are Supervisor and help from co-workers, lab equipment, software and budget.

**Chalmers**

Examiner

**E-sektionens Teletekniska Avdelning**

Mechanical workshop and other tools and equipment.

## 1.6 Course of action

Here a coarse description of the planned course of action in this project is presented.

- Prestudy of the inverters developed by QRTECH.
- Analysis of the safety and reliability needs
- Adaptation of the current hardware and software to this project
- Mechanical integration of the inverter
- Verification of the implementation
- Documentation

## 2 Electric Powertrain

In the automotive industry, the term powertrain refers to the system that generates propulsion. This includes the whole chain of components that generate power and delivers it to the road surface. In more detail, this means the engine, transmission, drive shafts, differentials and the wheels.

An electric vehicle (EV) is a vehicle that is powered, at least in part, by electricity. EV configurations include battery electric vehicles (BEVs) which are powered by 100% electric energy, various hybrid-electric vehicles (HEVs), and plug-in hybrid electric vehicles (PHEVs) [5].

An electric powertrain for a BEV may include everything of a traditional powertrain with the exception that a battery and some power electronic needs to be added instead of the liquid fuel tank, see figure 1 for an example. One advantage when using electric motors is that the need of using an external gear box is reduced since the torque and speed can directly be controlled by software, thus some kind of static transmission is often used to scale the max speed and torque between the engine and the drive shaft.

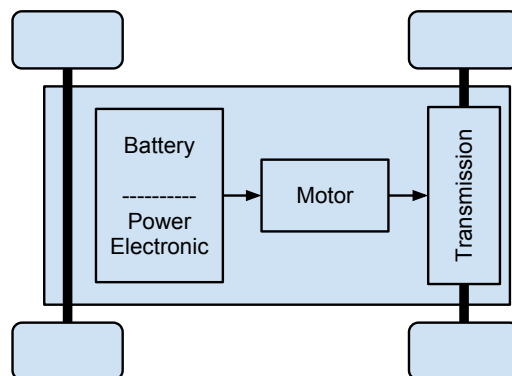


Figure 1: A simple example of an electric powertrain in a battery electric vehicle

### 2.1 Power Electronic Converters

Power electronic converters are used to process electrical energy. This means that when there is a need to modify one or many characteristics of the electrical energy like its voltage, current or frequency, these types of converters are used. In contrast to "classical" electronics like a radio or computer where the current and voltage are used to carry information, power electronics carry and process power, therefore the main metric becomes the efficiency.

The power conversion systems can be classified according to the type of the input and output power

- AC to DC (rectifier)
- DC to AC (inverter)
- DC to DC (DC to DC converter)
- AC to AC (AC to AC converter)

### 2.1.1 Space Vector Modulation

SVM is an algorithm for controlling PWM signals, and it is widely used for controlling switching power converters. A common application is the control of an inverter together with a 3-phase AC-motor. Figure 2 shows a 3-phase inverter that is supplied by a DC-source and loaded by a 3-phase AC-system. The SVM-algorithm outputs two PWM signals for each phase that controls the high and the low side of the halfbridge connected to that specific phase in the inverter. An important property of the algorithm is that it makes sure that at no time, both the high and the low side in the same half bridge are turned on. If both half's of a bridge were turned on at the same time, the DC supply would be shorted (ie. in 2, switch 1 may not be turned on when switch 4 is on). Therefore a dead-time is used between switching which side is on, to eliminate the risk of this.

Two important properties of SVM is that it transforms the rotating AC-quantity to a static DC-quantity, and gives the possibility to analyze and control the multi-phase system as a whole instead of looking at each phase separately. Both of these features simplify the control-loop. A three-phase system like the inverter described above where every phase is either turned on or off, leads to eight possible switching vectors. Six active switching vectors (V1 – V6) as seen in figure 3, and two zero vectors (V0, V7). The zero vectors describe the two states where all phases either are on or all phases are off). In the example when using an AC-motor, switching V1 through V6 would create a rotating magnetic-field as a cause of the current running through the windings in the motor, which would cause the shaft to revolve [6].

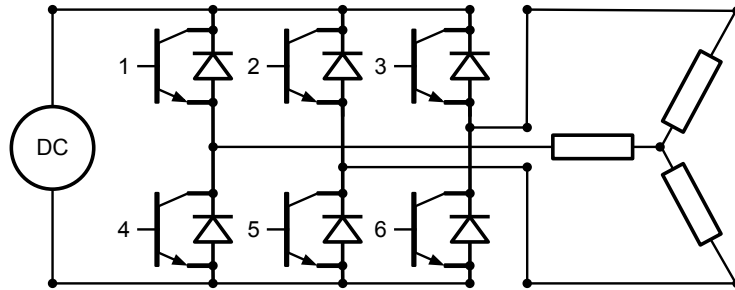


Figure 2: 3-phase inverter, with three half bridges connected to a load.

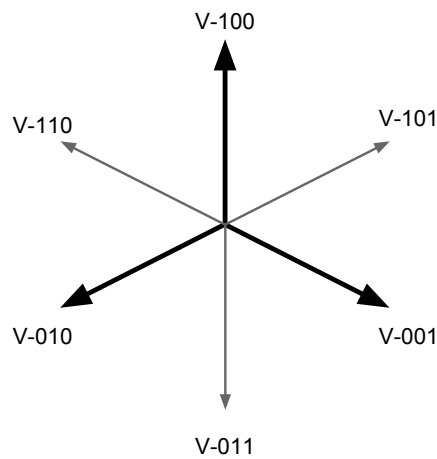


Figure 3: Space vector modulation vectors

## 2.2 Permanent Magnet Synchronous Motor (PMSM)

A synchronous electric motor is an AC motor that commonly consists of two basic parts, an outside stationary stator having coils supplied with an alternating current to produce a rotating magnetic field and an inside rotor with permanent magnets. The rotor is attached to the output shaft that is given a torque by the rotating field.

Synchronous motors can be contrasted with induction motors, which must

slip in order to produce torque. A PMSM operates synchronously with the AC frequency and the mechanical speed is determined by the number of pairs of poles and the frequency.

Most synchronous motors are used where precise constant speed is required. It is a highly efficient mean of converting AC energy to mechanical work and a PMSM can also be used as an alternator to regain energy when an external torque is applied to the motor.

## 3 System fault-tolerance and robustness

This section will describe the safety factors that the inverter will need to handle and how they are taken care of.

### 3.1 Analysis

#### **Current shoot-through**

The inverter must be built to ensure that no shoot-through currents can occur in any of the inverters half bridges.

#### **Heat**

The inverter must be able to handle the heat that the power components develop and have some protection in place to ensure that the hardware will not overheat and possibly sustain damage.

#### **Electrical Interference**

The inverter must be able to handle the interference itself and the motor produce during operation. However the inverter is not required to have EMC compliance with specifications such as those for CE-marking, since it is not required in this project.

#### **Torque cap**

The inverter must have a torque cap implemented so that the system will not provide more current than the inverter is built for, to ensure that the inverter itself or the motor it is driving will not sustain damage from over-current.

#### **Voltage drop**

The inverter must be able to handle voltage drops on the input power, since if the input voltage drops too much, control of the switching might fail due to some circuits not functioning properly.

### 3.2 Solutions

#### **Current shoot-through**

There are several safety features to deal with this demand. Software features ensure that both MOSFETs in any of the half bridges should not be turned on at the same time. As well as the gate drivers which have a hardware solution that ensures a minimum dead band in the switching and also never permits both transistors to be turned on simultaneously.

## Heat

This is an important consideration, since if the system is overheating, the circuitry might sustain damage and therefore multiple solutions has been implemented.

- Two types of sensors for measuring the temperature have been integrated
  - PTC resistors placed close to the half bridges on the power PCB, that at a max allowed temperature trigger an interrupt in the software that also automatically shuts down the gate driver hardware. This puts the PWM signals that control the inverter to a low state.
  - NTC resistor that is constantly sampled in the DSP to produce a temperature reading of the power PCB.
- A heat sink that is mounted directly to the power-board.
- A fan to cool of the sink. This is controlled by a linearly regulated PWM signal.
- A routine to reduce the torque if the heat sink and the fan is not enough to prevent the inverter from overheating.

## Electrical Interference

The whole inverter has been designed with this in mind. Most of the circuitry put in place to handle overshoots and oscillations are a part of the solutions to cope with this requirement. The layouts of both PCBs have many considerations in an effort to minimize noise and sensitivity to noise. These considerations and the component choices are described in much more detail in section 7.

## Torque cap

A torque cap has been implemented in software to ensure that the system will not provide more current than the inverter is built for.

## Driver Disable

Whenever the system or the user decides that the system should be disabled, the gate drivers that control the power PCB are switched off. This has two main positive effects; first, it will save energy since the drivers and the power PCB will stop switching; second is that if something is malfunctioning, some part might be damaged if continued switching is allowed.

## Voltage drop

This is taken care of by measuring the input DC-voltage from the battery. A minimum voltage is defined as a constant that is larger than

the minimum required voltage for proper functionality of the electrical components. If the measured voltage drops below this constant, the system will start to regulate against zero torque. There is also a constant lower than this which is the limit for when the controller will disable the drivers and stop switching. If the latter happens, a software interrupt occurs and the inverter is disabled, and will need to be reset for further operation.

## 4 System overview

In this section, a brief overview of the complete system is presented. The complete system designed in this project consists of a number of major parts which can be categorized as:

- Software.
- Electronic hardware.
- Mechanical hardware.

In figure 4 a block representation of the system electronics and software parts are presented to give a rough idea of how the system is designed.

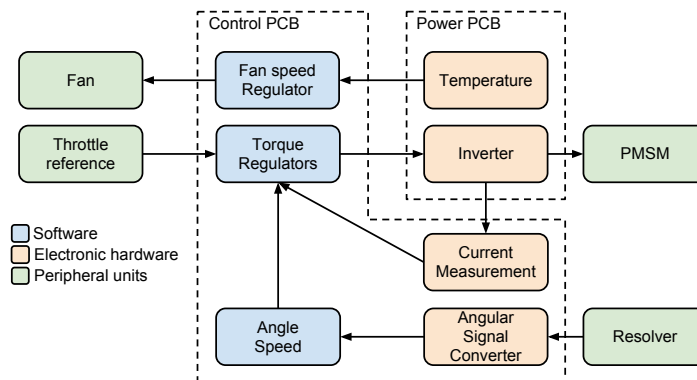


Figure 4: Block representation of the system electronics and software

The software contains the control loop and is running on a DSP. Inputs are read from the different sensors and the control loop generates the signals that controls the half bridges in the inverter. The software and its different parts are described in detail in sections 5 and 6.

The electronic hardware consists of two separate PCBs. One card for the actual power electronics such as the large power transistors in the half bridges. The other card houses the DSP, sensors and driver circuits that control the power electronics. The hardware solutions along with some component choices are described in detail in section 7.

The mechanical parts are the mounting solutions designed to enable the system to be implemented on QRTECH's go-kart together with for example cooling solutions for the inverter electronics. The mechanical parts designed in this project are described in detail in section 8.

## 5 Electronic Control Unit "ECU"

This chapter will describe a general theory behind an ECU for motor control and its sub blocks. It consists of routines for collecting and processing data from the inverter and peripheral units as well as controlling them, it handles security and log data.

This section will not describe how the ECU interfaces to other units nor give a detailed description of the software implementation since that is specific to this project. Those parts is discussed in section 6.

### 5.1 Torque Control Loop

The torque control loop is the most central part of a motor control system, this is the part that controls the PMSM through switching the inverter board. Its main purpose is to regulate the input to the PMSM so that the torque increase and decrease will feel smooth, be safe and at the same time be as fast as possible without overshoots.

An overview block diagram of the complete loop is shown in figure 5.

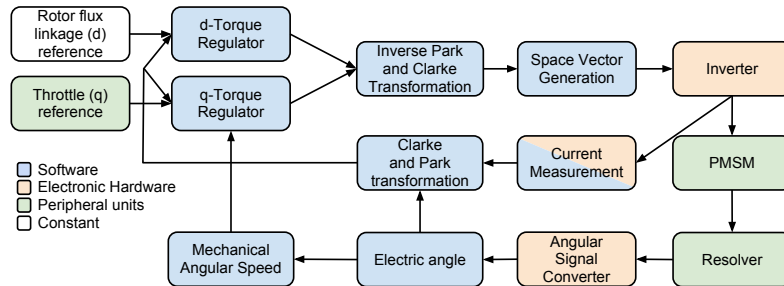


Figure 5: An overview of the torque control loop

#### 5.1.1 Current Measurement

The current measurement uses two equations, one for calculating the actual current and one for calibration. The calibration calculates an *offset* that represents zero current. This is done using equation 1 for all 3 phases, where  $x$  is an arbitrary picked number and  $I_{MEAS}$  is the measured current.

$$I_{offset} = \frac{1}{x} \times \sum_{i=1}^x I_{MEAS}(i) \quad (1)$$

Equation 2 calculates the actual current, this is done for all 3 phases.

$$I = (I_{MEAS} - I_{offset}) \quad (2)$$

### 5.1.2 Electrical Angle

The electrical angle is used as a feedback to know where the motor-shaft is positioned. This information is used to calculate speed and as an input to the space vector modulation. There is a number of ways to calculate the angle and the one used in the project is described in section 6.2.

### 5.1.3 Mechanical RPM

The mechanical RPM is calculated using equation 3 on the electrical angle ( $\theta$ ) described in section 5.1.2. The difference between mechanical and electrical RPM is the number of pole pairs in the motor, the electrical RPM describes how fast the magnetic field in the motor is rotating in contrast to mechanical RPM which describes the speed of the motor shaft. The sample time ( $t$ ) is in seconds which is why the  $\Delta\theta$  is multiplied by 60 and *PolePairs* refers to the amount of pole pairs in the PMSM.

$$v_{mech} = \frac{(\Delta\theta) = \theta_0 - \theta_{-1}}{t \times PolePairs \times 2\pi} \quad (3)$$

### 5.1.4 Clarke transformation

The  $\alpha\beta$  transformation, or the Clarke transformation, is used to simplify the analysis of three-phase system using equation 4. Figure 6 shows how  $\alpha$  and  $\beta$  corresponds to the three phases.

[7] [8]

$$\begin{cases} s_\alpha = s_a \\ s_\beta = \frac{s_b - s_c}{\sqrt{3}} \end{cases} \quad (4)$$

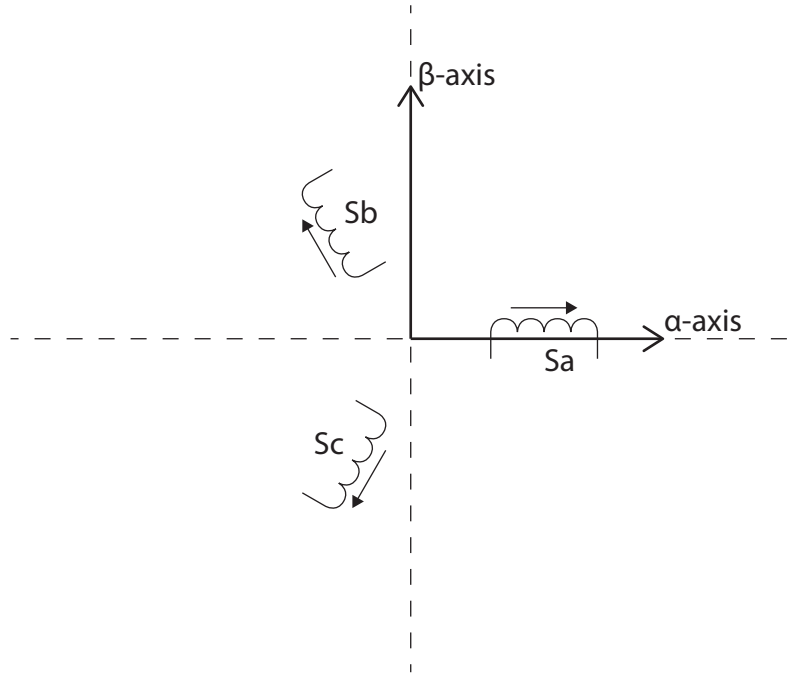


Figure 6: Shows  $S_{abc}$  in relation to  $S_{\alpha\beta}$

With a symmetric load, equation 5 is true and therefore equation 4 can be reduced to equation 6.

$$0 = s_a + s_b + s_c \quad (5)$$

$$\begin{cases} s_\alpha = s_a \\ s_\beta = \frac{s_a + 2 \times s_b}{\sqrt{3}} \end{cases} \quad (6)$$

Clarke's inverse transformation is shown in equation 7.

$$\begin{cases} s_a = s_\alpha \\ s_b = \frac{-s_\alpha + \sqrt{3} \times s_\beta}{2} \\ s_c = \frac{-s_\alpha - \sqrt{3} \times s_\beta}{2} \end{cases} \quad (7)$$

### 5.1.5 Park's transformation

The dq transformation, or Park's transformation, converts the two AC quantities ( $\alpha$  and  $\beta$ ) to two DC quantities (*direct* and *quadrature*). This sim-

plifies the use of these quantities as feedback input to the regulators. The  $d$  and  $q$  representation is achieved using equation 8 where  $\theta$  is the electrical angle described in section 5.1.2 [7] [8].

$$\begin{cases} s_d = s_\alpha \times \cos(\theta) + s_\beta \times \sin(\theta) \\ s_q = -s_\alpha \times \sin(\theta) + s_\beta \times \cos(\theta) \end{cases} \quad (8)$$

Park's inverse transformation is shown in equation 9.

$$\begin{cases} s_\alpha = s_d \times \cos(\theta) - s_q \times \sin(\theta) \\ s_\beta = s_d \times \sin(\theta) + s_q \times \cos(\theta) \end{cases} \quad (9)$$

### 5.1.6 $d$ - and $q$ -torque regulators

In the torque control loop the system regulates two DC quantities ( $d$  and  $q$ ). There is one independent regulator for each quantity. The measured current is transformed as described earlier and used as feedback. The  $d$  quantity is used to control the rotor flux linkage while the  $q$  quantity is used to control the torque. This project is only focused on controlling the motor torque and therefore this system uses a static 0 reference for the  $d$  quantity. The  $q$  quantity however gets its reference from the throttle, for further details, see section 6.3.

In the regulator for the  $q$  quantity there are also two built-in safety parts:

- Decrease torque reference if the measured mechanical speed has reached an upper allowed limit.
- Decrease torque reference if the measured temperature of the power PCB has reached an upper allowed limit.

An overview block diagram of the  $q$ -torque regulator can be seen in figure 7.

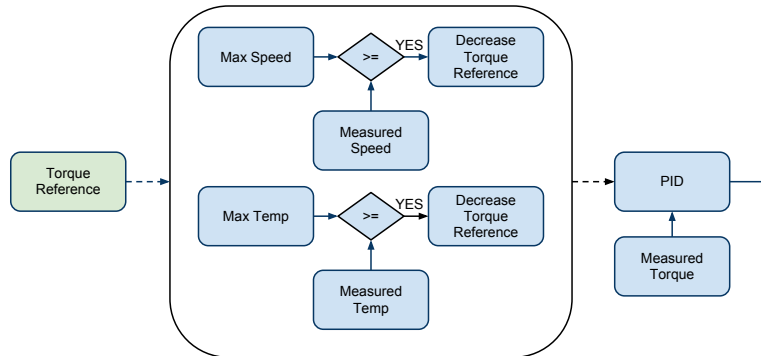


Figure 7: An overview of the  $q$ -torque regulator

### 5.1.7 PID

A Proportional Integral Derivative controller (PID controller) calculates an "error" value as the difference between a measured process variable and a desired setpoint. The controller attempts to minimize the error by adjusting the process control inputs.

A general implementation of a PID-controller can be seen in figure 8.

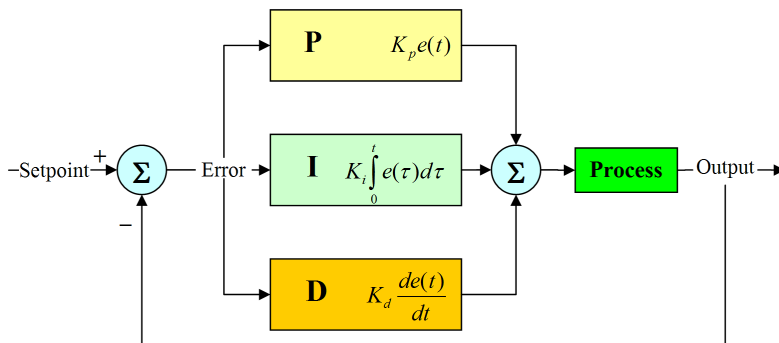


Figure 8: A simple block-diagram of a continuous PID-controller[9]

### Ziegler-Nichols method

The Ziegler-Nichols method is a method used to optimize a PID-controller. This method is especially good and simple to use when the process response is unknown. The downside is that it can render a rather unstable controller [10].

The method is carried out as follows:

- Turn off the I- and D-parts, ie. set  $T_i = \infty$  and  $T_d = 0$ .
- Set  $K_0$  to 0.
- Then increase  $K_0$  iteratively until the system begins to oscillate.
- Measure the period time  $T_0$  as in figure 9.
- Adjust the parameters according to table 1.

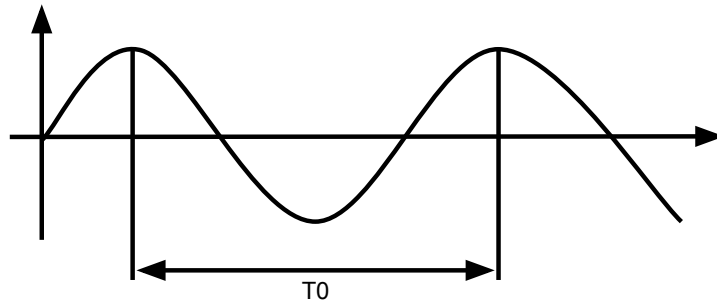


Figure 9: Ziegler-Nichols

Type	Parameters		
	$K$	$T_i$	$T_d$
P-type	$0.5K_0$	—	—
PI-type	$0.45K_0$	$0.85T_0$	—
PID-type	$0.6K_0$	$0.5T_0$	$0.125T_0$

Table 1: Ziegler-Nichols

However Karl Johan Åström and Tore Hägglund have shown that when using the same method, the parameters chosen in table 2 normally leads to a better stability [10]. Therefore the PID controllers were configured using this method.

Type	Parameters		
	$K$	$T_i$	$T_d$
PID-type	$0.35K_0$	$0.77T_0$	$0.19T_0$

Table 2: Åström - Hägglund

### 5.1.8 Sector Calculations

This section describes the part that calculates the duty cycle  $t$  that is used to generate PWM signals to control the halfbridges in the inverter. The first thing is to convert the DC quantity ( $d$  and  $q$ ) back to a 3-phase AC quantity using the inverse Park-transformation, see equation 9 and the inverse Clarke-transformation, see equation 7.

Table 8 is then used to find the equation to calculate the correct duty cycles for the three phases in the inverter. This table is used to simplify the calculations that would otherwise be needed. A degree interval for every sector can be seen in the table, except for sector 0 and 7 which represents the case when the output power from the inverter is zero.

<b>Sector 0:</b> $t_a = 0.5$ $t_b = 0.5$ $t_c = 0.5$	<b>Sector 1:</b> 90 - 150 degrees $t_a = (1.0 - U_a - U_b)/2.0$ $t_b = (1.0 - U_a + U_b)/2.0$ $t_c = (1.0 + U_a + U_b)/2.0$
<b>Sector 2:</b> 150 - 210 degrees $t_a = (1.0 - U_b + U_c)/2.0$ $t_b = (1.0 + U_b + U_c)/2.0$ $t_c = (1.0 - U_b - U_c)/2.0$	<b>Sector 3:</b> 210 - 270 degrees $t_a = (1.0 + U_a + U_c)/2.0$ $t_b = (1.0 - U_a - U_c)/2.0$ $t_c = (1.0 + U_a - U_c)/2.0$
<b>Sector 4:</b> 270 - 330 degrees $t_a = (1.0 - U_a - U_b)/2.0$ $t_b = (1.0 - U_a + U_b)/2.0$ $t_c = (1.0 + U_a + U_b)/2.0$	<b>Sector 5:</b> -30 - 30 degrees $t_a = (1.0 - U_b + U_c)/2.0$ $t_b = (1.0 + U_b + U_c)/2.0$ $t_c = (1.0 - U_b - U_c)/2.0$
<b>Sector 6:</b> 30 - 90 degrees $t_a = (1.0 + U_a + U_c)/2.0$ $t_b = (1.0 - U_a - U_c)/2.0$ $t_c = (1.0 + U_a - U_c)/2.0$	<b>Sector 7:</b> $t_a = 0.5$ $t_b = 0.5$ $t_c = 0.5$

Table 3: Sector calculations

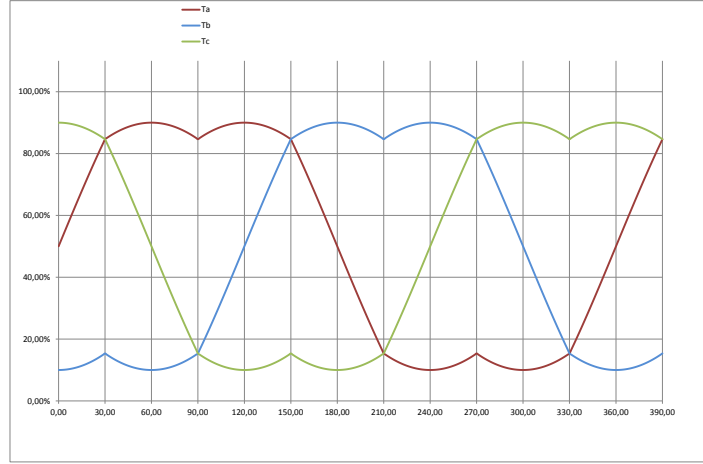


Figure 10: Output from the space vector generation during different angles when the torque reference is 80%

## 5.2 Fan Controller

This ECU uses both passive and active cooling in terms of a heat sink (more in section 8.1) and a fan. Table 4 describes how the fan is controlled. To save energy an "on" temperature was defined to when the fan should begin rotating, it is also set as the target temperature. For the algorithm a "max" temperature was defined to when the fan should rotate at maximum speed.

$T_{Feedback}$	$\omega$
$> T_{MAX}$	$\omega_{MAX}$
$< T_{ON}$	<i>OFF</i>
$> T_{ON}$	$\omega = \omega_{ON} + \frac{(\omega_{MAX} - \omega_{ON}) \times (T_{Feedback} - T_{ON})}{T_{MAX} - T_{ON}}$

Table 4: Table showing how the speed of the fan is controlled depending on the measured temperature.  $\omega_*$  and  $T_*$  are constants.

## 6 DSP and software specific to this project

This section describes the DSP used in this project and what application specific software that has been constructed for this micro controller and the custom PCB.

### 6.1 DSP - TMS320F28335

The DSP is a part of the Texas Instruments C2000 family and was provided by QRTECH. It has been chosen as a generic development platform because of its floating point acceleration and large range of integrated peripheral modules (CAN, ADC, PWM etc.). The modules used in this project are described in this section, but this DSP has a larger range of peripheral modules built-in that can be used in different applications. This section gives a short description of the DSP that was used, further reading for more detailed descriptions can be found in the datasheet [11].

#### **ADC-module**

This DSP has a built-in 12-bit ADC-core which can sample up to 12.5 MSPS. It has 2 Sample/Hold circuits and 16 dedicated ADC channels where 8 channels can be multiplexed per Sample/Hold. It has an auto sequencing capability that provides up to 16 "auto-conversions" in a single session. Each conversion can be programmed to select any of the 16 input channels. A session can either be triggered by software or the PWM-module.

#### **CAN-module**

The CAN module is fully compliant with CAN protocol, version 2.0B and supports data rates up to 1 Mbps. It also has 32 mailboxes with up to 8 bytes of data each.

#### **GPIO-module**

The device supports 88 GPIO pins, but all pins are multipurpose in the sense that they can support one or more peripheral modules as well. Two examples are that GPIO-0 also can be used as PWM channel 1-A and GPIO-12 can also can be used as either Trip Zone-1 or CAN-B transmit.

#### **PWM-module**

The PWM-module has 12 channels divided on 6 pairs, the system has 6 dedicated Trip-zone signals to alert the module of external fault condition. What happens when different trips occur can be configured individually for every pair of PWM-channels. The PWM-module can also be used to start internal interrupt sequences and ADC-conversions.

### QEP-module

The quadrature encoder pulse (QEP) module is used for direct interface with a linear or rotary incremental encoder to get position, direction, and speed information from a rotating machine. In this project it takes two pulse trains (A and B) where every pulse represent a fraction of the revolution, it combines this with a third pulse train (I) that ticks once every full revelation.

### Real-Time JTAG and Analysis

The device implements the standard IEEE 1149.1 JTAG interface and supports real-time analysis whereby the contents of memory, peripheral and register locations can be modified while the processor is running and executing code and servicing interrupts. The user can also single step through non-time critical code while enabling time-critical interrupts to be serviced without interference. Additionally, it allows setting of hardware breakpoint or data/address watch-points.

## 6.2 Electric Angle from pulsetrain

The signals from the IC-circuit described in section 7 is fed to the QEP module and then equation 10 is used where  $POSCNT$  is the current partial length of an electric revolution in the PMSM,  $CPM$  is the total length of an electric revolution,  $2.0 \times \pi$  is to transform it into radian and  $calibratedAngle$  is the static phase shift between the PMSM and the Resolver. The QEP-module can be used in a number of ways to calculate the position count, in this application the flanks of the A-pulse train triggers an up-count of the  $POSCNT$  and the I-pulse train resets it to zero.

$$\theta = \frac{2.0\pi \times POSCNT}{CPM} + calibratedAngle \quad (10)$$

## 6.3 Torque Reference

This project uses a potentiometer for determining the torque reference and this chapter will discuss the implementation of this. The ECU also has built-in functionality to be able to receive a torque reference from a Master through CAN.

### 6.3.1 Potentiometer

To get a torque reference ( $\tau_{REF}$ ) from the driver, two potentiometers are used, one for acceleration ( $AccRef$ ) and one for the brakes ( $BrakeRef$ ). To

ensure that the motor will not output a too high torque when the mechanical brake is applied, equation 11 is used to reduce the accelerator's impact. The reason for this is that one might otherwise burn power unnecessarily or burn the windings in the motor. One aim here is that the brakes should have little or no impact on the motor when a low force is applied and have an impact growth that is polynomial, where the brakes will cut off the accelerator when they are applied by 50%. *AccRef* and *BrakeRef* are normalized values between 0.0 to 1.0.

$$\tau_{REF} = (AccRef - 32 \times BrakeRef^4) \times \tau_{MAX} \quad (11)$$

#### 6.4 Temperature measurement

The temperature measurement is done by a thermistor of a nonlinear NTC-type, the details of this can be found in the datasheet [12]. Because this is nonlinear, some kind of linearization needed to be carried out for the DSP to be able to convert the ADC-readout ( $x$ ) to an approximated temperature. Two methods were considered, lookup-table and multiple equations for short intervals. Look-up tables (LUT) lost because recalculating the ADC-readout to an address that could be used with a LUT would be more complex than to use the hardware acceleration for floating point multiplications in the DSP. And this renders it faster to use multiple equations with a switch and case statement which is important since the calculation is executed during the interrupt-loop which has a given time frame. This resulted in 6 first order equations, see equation 12 and their results can be seen in table 5. The reason for multiplying with 4095 in equation 12 is that this equation is written so that it can easily be modified from taking normalized input from 0.0 - 1.0 to the real ADC-readout where 1.0 is represented by 4095.

In table 5, the deviation from the real temperature to the calculated one is always less than  $1^\circ C$ , these equations were auto generated and the effort to produce these 6 equations were therefore negligible. These precise values are not of a great importance when controlling the fan, but the values are supposed to be presented to the driver and used for future development and optimizations, and thus the seemingly unnecessary precision.

$$t = \begin{cases} -0.0256 \times 4095 \times x + 103.82, & 1.000 \geq x > 0.828 \\ -0.0213 \times 4095 \times x + 90.263, & 0.828 \geq x > 0.493 \\ -0.0253 \times 4095 \times x + 98.389, & 0.493 \geq x > 0.308 \\ -0.0377 \times 4095 \times x + 114.83, & 0.308 \geq x > 0.211 \\ -0.0627 \times 4095 \times x + 135.11, & 0.211 \geq x > 0.128 \\ -0.1083 \times 4095 \times x + 157.63, & 0.128 \geq x \geq 0.000 \end{cases} \quad (12)$$

real ( $^{\circ}C$ )	aprox. ( $^{\circ}C$ )	real ( $^{\circ}C$ )	aprox. ( $^{\circ}C$ )
10,00	9,66	70,00	70,31
15,00	14,42	75,00	75,55
20,00	20,27	80,00	80,22
25,00	25,00	85,00	84,39
30,00	29,94	90,00	90,40
35,00	34,99	95,00	95,67
40,00	40,04	100,00	100,31
45,00	44,58	105,00	104,35
50,00	50,14	110,00	110,41
55,00	55,35	115,00	115,61
60,00	60,16	120,00	120,27
65,00	64,54	125,00	124,27

Table 5: Real values and their respective approximated values from the model used.

## 7 Hardware

In this section the inverter hardware and its components will be discussed. At first a brief overview of the system will be presented and then the function will be described. The most relevant and active component choices made in this project will be discussed and motivated here and the physical solution with layout will be discussed. Throughout this chapter it is valuable to have the schematics for the two parts of the system at hand. The schematics, together with drawings of the layouts, can be found in appendix A and B.

### 7.1 Hardware overview

The complete system has two major parts, the control PCB and the power PCB. The power PCB contains the half bridges and the actual inverter as such. The control PCB contains all the parts necessary to ensure the functionality of the power PCB. That is, the DSP, sensors, the gate driving for the half bridges and some miscellaneous devices for communication. Therefore the main focus here will be on describing the control PCB, since the power PCB mostly contains the half bridges for the inverter. In figure 11 a block scheme of the control PCB can be found. Below the description of the parts and their functionality is presented.

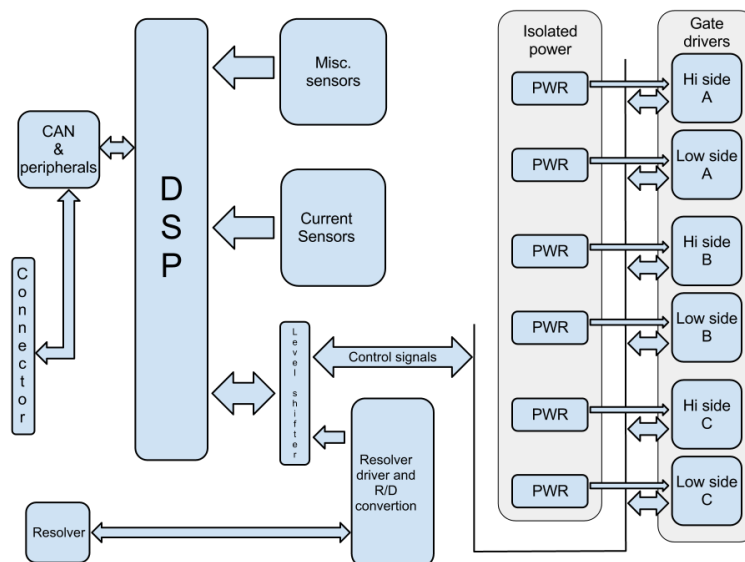


Figure 11: Block schematic of the hardware in the control system

## 7.2 Description of the system blocks

Here a more in-depth description of the system blocks can be found. The general function is described for each of the blocks and the design is discussed. For reference see the schematics in appendix A and B.

### 7.2.1 CAN & peripherals

In this block the CAN controller and some outputs for peripheral indicator LEDs are found. CAN is implemented with a basic CAN transceiver and some ESD protection on the bus terminals. The CAN transceiver is then directly connected to the on-board CAN controller in the DSP. The outputs for the indicator LEDs are driven by small MOSFETs in series with a current limiting resistor. The outputs are connected to the cathode of standard LEDs.

### 7.2.2 Current sensors, resolver and miscellaneous sensors

On the control PCB some different sensors are implemented. The most prominent ones on the PCB are the three current sensors that measure the current output to each of the three phases. These are operation critical and are hall-effect type current sensors from LEM that can measure up to 300A. The sensors outputs a voltage directly proportional to the current flowing through the sensor. Since the sensors are supplied with 5V the output ranges from 0 to +5V. The DSP can only handle +3.3V on the ADC inputs though, this is sorted by a simple resistive voltage divider. This could have been solved with a op-amp instead, which would have been a much more proper solution, however this would have required too much time to develop. Therefore the simple solution was preferred. The sensors also have simple RC-low pass filters on the outputs to reduce the high frequency noise on the signal to the DSP.

The other operation crucial sensor is the angle sensor mounted on the motor. This sensor is a resolver type sensor, and the sensor itself is described in detail in section 8.4. This sensor measures the angle of the motor drive shaft in electrical RPM. This means that the output angle from the sensor is directly coupled to the current flowing through the motors windings. Both the motor and the resolver sensor thus have four electrical revolutions per mechanical revolution. The resolver requires a driving and conversion circuit, which drives the primary side of the resolver and converts the outputs from the resolver sensor to either a 12bit binary number or to two pulse trains and an index pulse, equivalent to the outputs of an encoder. In this project the encoder equivalent outputs were chosen since the DSP has an

integrated module to decode such an input to an angle. This also reduces the number of I/O lines required on the DSP. The R/D converter IC also outputs the sine and cosine waveforms and these are also connected to the ADC unit in the DSP via a resistive voltage divider. This was done to enable the future development of a software R/D converter, however this is not in the scope of this project.

On the power PCB there are two types of temperature sensors. Firstly there is an NTC resistor to measure the actual temperature of the power PCB and the heat sink. Secondly, there is also a series of PTC-resistors, with one resistor for each half bridge. These are used to disable the inverter via hardware shutdown functions to prevent damage due to overheating. The chain of PTC-resistors is connected to an op-amp based comparator with a small window of hysteresis. The output of the comparator is connected to the hardware shutdown on all of the gate drivers and to a GPIO on the DSP to indicate normal operating temperature. The same signal is also, via a small transistor, connected to the DPS's shutdown signal, to enable the software to utilize the hardware shutdown on the drivers.

### 7.2.3 Gate drivers

Each phase has a set of gate drivers which drive the gates of the MOSFETs in the bridge. Since this inverter needs to be able to handle large amounts of current, there is a demand for low resistive losses and ability for fast switching of the transistors. This set of demands makes P-channel MOSFETs undesirable since they have much lower charge carrier mobility and thus need to be a lot bigger to compensate this and meet the current requirement. This in turn leads to an equal increase in gate capacitance. However, the N-channel device needs a positive gate-source voltage to be turned on, and this is the reason for the use of galvanically isolated gate drivers.

The gate drivers used for this design are the Infineon 1ed020i12-f isolated drivers. These gate drivers were prechosen to this project by QRTECH. Each gate driver drives one side (upper or lower side) of each phase, thus there are two drivers per phase and six drivers in total in the design. Input to the drivers are isolated power, and control signals. Among the controls signals there are two PWM signals, one for the upper half and one for the lower half of the phase, i.e. the two drivers in each phase receive the PWM signals for both the upper and the lower half of the phase that they are driving. This is done because built in to the drivers is a safety feature that by the use of both PWM signals ensures that both half's of a bridge is never in on state at the same time and thus preventing shoot through currents. A shutdown or reset input is also available which turns off the

driver output. This is used either by the software or by the temperature protection to shut down all the gate drivers if needed.

On the output side of the drivers there are small driving bridges, that consists of a pair of npn/pnp bipolar transistors, two for each half bridge (see schematics in appendix A for details). By this design the gate drivers only have to drive a signal to the final small bridges that do the actual driving of the MOSFETs gates. Although the drivers are specified to drive 2A rail to rail[13], these small final bridges were implemented. When this is done the driver only needs to drive the output to signal strength, and the actual drive current to the gates are delivered by the final small npn/pnp bridges. This design offers very high noise immunity since the drivers can drive their output very hard. The final small bridges also have a small filtering of the power supplied to the bipolar transistors with a  $100\Omega$  resistor and a  $1\mu\text{F}$  capacitor. Since the gates are more or less a capacitor that is charged to turn the MOSFET on, the large capacitor and the resistor smooths out the current spikes that otherwise would appear on the supply lines to the small bridges. This is desirable since it reduces noise emissions.

#### **7.2.4 Isolated power**

The gate drivers need a galvanically isolated power supply to drive the MOSFETs. The power is supplied by Traco isolated power modules that output galvanically isolated 24V. This is then divided with zener diodes to give a +15V, -8V and a GND reference. By dividing the isolated voltage the gates of the MOSFETs can be driven to voltages that ensure safe and reliable operation. By driving the gates to -8V in off state, the possibility of the transistor being turned on from over heard noise to the gate, or by parasitic capacitances is greatly reduced.

#### **7.2.5 Half brigdes**

The half bridges are the main part of the inverter it self, see schematics in appendix B. They mainly consist of a pair of MOSFETs connected in series between the poles of the battery supply. The output phase voltage is connected in between the two transistors. Parallel to each of the transistors snubber circuits are connected. The snubber is a RC-circuit used to dampen overshoots that occur from the parasitic inductance in the tracks on the power PCB. The snubber is further discussed in section 7.3.4. In parallel with both the transistors is the reverse recovery capacitor connected, this is also discussed in detail in section 7.3.3. To the gate of each MOSFET there is a protection diode connected to protect the transistor from a too high gate voltage. There is also a small transistor connected between the gate

and the source on the large MOS devices. This transistor is there to ensure that the gate of the large MOSFET is kept low when the device is turned off and does not get turned on by parasitic capacitances or other noise. The signals to control this are connected to the control PCB via a 6 way pin header.

### **7.3 Component choices**

In this section the major important component choices are discussed in detail. Many of all the components used in the whole design are not discussed here since many are considered self explanatory, such as pull up/down resistors and decoupling capacitors. Those components of interest are more of a crucial nature to the design and have been changed from the original design to fit the new specification. Note that the whole design is mostly carried over from a previous similar project with another set of demands on voltages and currents and thus most of the design choices were not made in this project.

#### **7.3.1 Traco power modules**

To supply the isolated gate drivers with galvanically isolated power, Traco power modules were chosen. In the original design, this isolated power was supplied via switch transformers controlled by the DSP. This solution needed some rework to handle the increase in power demand when redesigning from IGBTs to MOSFETs used in this project, since the IGBTs from previous design has a much lower gate charge than the MOSFETs and there were fewer of them. Thus the demand for current is increased. However due to time constraints and a desire to simply avoid problems arising from these power supplies a complete off the shelf solution was chosen. The modules take an input voltage of 36-72V and outputs an galvanically isolated 24V, 125mA.

#### **7.3.2 MOSFET transistors**

The MOSFET transistors chosen for the inverter are from the OptiMOS 3 power transistor series from Infineon. The specific transistors chosen have the following general specifications:

Description:	value:
$V_{DS}$	100V
$R_{DS(on),max}$	2.5m $\Omega$
$I_D$	180A

Table 6: Basic properties of the MOS-transistors

Infineon was prechosen as supplier of the transistors for this project by QRTECH. The choice of the specific transistor was however made in the scope of the project. According to the specifications the inverter needs to be able to handle 300A peak current. Due to the large peak current, a decision to go with three half bridges per phase, rather than one or two, was made. When handling the large peak current, the thermal aspect of the design becomes very important. The maximal junction temperature the transistors can handle is 175°Celsius[14]. This temperature must not be exceeded in order to avoid damage to the transistors. In this calculation the peak current is used rather than the RMS current. This is done because of two main reasons. This ensures a good safety margin during normal operation which is desirable since the inverter is a prototype. It also takes in to account the case where the motor does not rotate and full throttle is applied, in this case the transistors must be able to handle the peak current during a prolonged period of time. The heat transfer to the surrounding air can be calculated according to equation 13 where  $R_\theta$  is the sum of the absolute thermal resistances of the different junctions and  $Q$  is the thermal power that flows through the system [15].

$$\Delta T = Q \times R_\theta \quad (13)$$

Where  $\Delta T$  can be written as:

$$\Delta T = T_{junction} - (T_{Ambient} + T_{Heatsink}) \quad (14)$$

And  $Q$  is the the thermal power generated by one of the transistors, calculated as:

$$Q = R_{ch} \times I_{DS}^2 \quad (15)$$

The inverter is specified for a peak current of 300A, to be able to handle this current with a reasonable amount of resistive losses on the MOSFETs, a

decision was made to go with three half bridges/phase and thus  $I_{DS} = 100A$  for each half bridge. Thus the current through each half bridge is reduced to a third, which will reduce the resistive losses to  $1/9$ . The thermal resistances combined in the term  $R_{\theta}$  are all the different layers and junctions between the transistor itself and the surrounding air. The different absolute thermal resistances are found in table 7. Note that a compensation has been assumed to account for the junction between the heat sink and the aluminum PCB where the power components are mounted.

Description:	value [ $^{\circ}C/W$ ]:
$R_{junction}$	0.5
$R_{Al-PCB}$	0.45
$R_{Heatsink}$	0.34
$R_{comp}$	0.3
Sum	1.59

Table 7: The different absolute thermal resistances connected to the MOSFETs in the inverter

In this case the ambient temperature was assumed to be  $30^{\circ}C$  and the heat sink was assumed to be kept at no more than  $30^{\circ}C$  above the ambient temperature. Combining equations 13, 14 and 15 and then solve for  $R_{ch}$  :

$$R_{ch} \leq \frac{175 - (30 + 30)}{(0.5 + 0.45 + 0.34 + 0.3) \times 100^2} \simeq 7.2m\Omega \quad (16)$$

The allowable channel resistance of the MOSFET is then less or equal to  $7.2m\Omega$ . This requirement must be fulfilled even when the junction temperature has risen to near the allowable temperature ( $175^{\circ}C$ ). The chosen transistor has a  $R_{ch} \simeq 5.4m\Omega$  when  $T_j = 175^{\circ}C$ . It is important that the channel resistance is within allowable limits even in the worst case when the junction temperature in the transistor is high.

### 7.3.3 Reverse recovery capacitors

When the body-source diode in a MOSFET has been forward biased and the transistor is shut off, the diode will be backwards biased. For a short while the body source diode will suffer from what is known as reverse recovery though. When this occurs, charge from the pn junction must be removed to form the depletion region in the diode. This appears as if the diode is conducting for a short while. In this case the reverse recovery charge is  $232nC$ [14]. A capacitor is placed between the  $V_{DD}$  and  $V_{SS}$  of each half

bridge, as close as possible to the transistors, to handle this charge. The capacitor must be a ceramic or plastic, since the the course of the reverse recovery is in the order of 10th of nano seconds. The chosen capacitor is of X7R-type dielectric. The accepted voltage ripple over this capacitor when this charge flows in and out of the capacitor was set to 0.05V. The required capacitance to achieve this is then:

$$C = \frac{Q}{V} = \frac{232nC}{0.05V} \simeq 4.7\mu F \quad (17)$$

In the inverter two of these capacitors have been stacked for double the capacitance. This was done to further decrease the amplitude of the ripple on the  $V_{SS}$  and  $V_{DD}$  rails to the half bridges.

#### 7.3.4 Snubber circuit

The "snubber" is a RC-link placed parallel to each MOS-transistor in all the half bridges. The snubber circuit is there to handle the voltage overshoot that occurs when the MOS-transistors are turned off. This overshoot occurs due to the stray inductance, that comes from the cables and the tracks on the power PCB and such, which tries to continue driving the current though the transistor when it is quickly turned off.

As a rule of thumb, a RC-snubber for a MOSFET can be designed with a capacitance twice the output capacitance of the transistor. The resistor value is determined by measuring the frequency of the oscillations on the overshoot, and then fitting the cutoff frequency of the RC-link to the frequency of the oscillations. In this design however, the capacitance was chosen to be able to handle as much energy as possible to minimize the peak voltage of the overshoot, and was therefore chosen to 22nF, since these capacitors were already available.

To decide the resistor value in the RC-link, the max current though the transistor was considered. When driving the max allowed 100A, and abruptly shutting off the transistor, the current will continue flowing for a short while. This current will flow through to the capacitor, and since the capacitor is conducting like this, basically the whole voltage drop will end up over the resistors. This voltage is simply derived from ohm's model in equation 18.

$$U = R \times I \quad (18)$$

The voltage over the resistor needs to be sufficiently low to not break the resistor. The accepted voltage over the resistor was decided to be less than

100V but the resistor can not be too small since this would cause unnecessarily large amounts of energy being wasted as heat. Therefore after some discussions the resistance was chosen to  $0.68\Omega$ . This will give a voltage of 68V when 100A flows through the snubber, which was deemed as acceptable.

## 7.4 PCB Layout

In this section the configuration of the PCBs and layout of both of the PCBs will be discussed. Some special considerations and component placement will be discussed. The section is divided into one chapter per PCB. The inverter PCBs are divided in to a power PCB where the half bridges are mounted and a control PCB where the DSP and the gate drivers are mounted.

### 7.4.1 Power PCB

The power PCB is a aluminum substrate type PCB. This is necessary since the chosen transistors are surface mounted and they require cooling to not overheat. This type of PCB only permits one copper layer to route the design. The layout of the power PCB is basically shaped like a ring. This design was chosen rather than a design with each of the phases in a straight line. This straight line design had been tested in a previous design for an

inverter for the go-kart, though the results were not optimal. Over all, the half bridges are arranged in a circular pattern, where the battery connections are placed outwards and the output or the phase connections are placed inwards. Since there are three half bridges per phase, there are a total of nine half bridges in the design, and they are arranged alternating between the three phases. That is, they are ordered as phase: A-B-C-A-B-C-A-B-C following the circle around.

Outside the half bridges two 3mm thick copper rings are placed to carry the input power from the battery to each of the half bridges. It was clear from the linear design that first of all the reverse recovery capacitor needed to be placed very close to the transistors in each half bridge due to the huge current spikes that these capacitors need to handle. Thus the inductance of the copper trace (or the wire) to these capacitors must be kept to an absolute minimum.

In the design chosen for this project the transistor pair for each half bridge are placed next to each other and the reverse recovery capacitor is placed directly between the connections between the transistors and the input power rails. The trace length between the gate on each MOSFET and the connector to the control PCB, including trace length for the small transistor connected between the gate and source on the large transistors, also needed

special care. These traces need to be as short as possible to have as low impedance as possible and to avoid picking up too much noise, which could lead to potentially driving a transistor to a faulty state.

The old linear design also had a large input capacitor for some current buffering, though it had become apparent that the trace length from the half bridges out to the large capacitor was too great. With this in mind a large number of smaller aluminum electrolytic capacitors were placed on the copper rings. This enabled the capacitance to still be quite large and yet be distributed over all the half bridges, and thus the trace length to the bridges is minimized.

A picture of the finished power PCB, fully populated can be seen in figure 12.

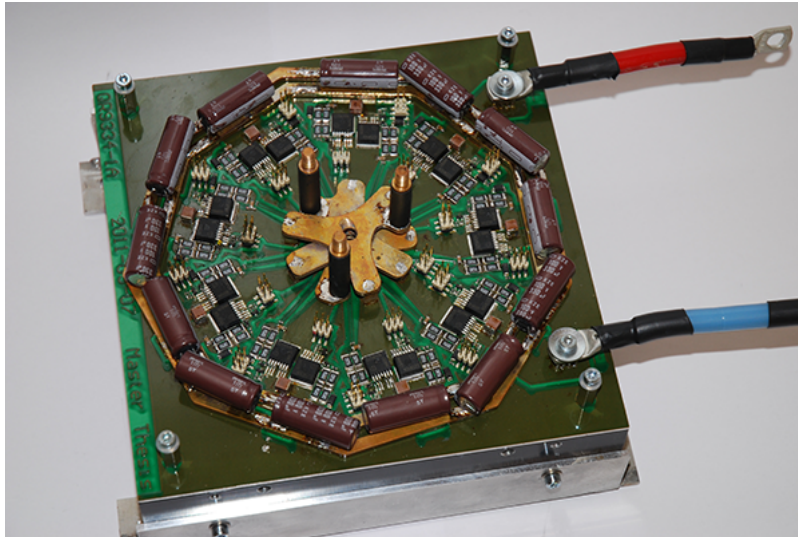


Figure 12: The finished power PCB mounted on the heat sink

This PCB was the first to be routed since it has most of the components with routing requirements that is to be considered critical. One of the half bridges was initially routed and then the routing was copied over to the other 8 half bridges. All the bridges were then arranged in the circular pattern and finally the temperature and overheating sensors were placed and routed.

#### 7.4.2 Controller PCB

Before any component placement or routing was made, the PCB stack-up was decided as follows:

- 6 layers should be used. This was preferred to save time spent routing compared to a 4 layer board
- All components must be placed on the top layer, with exception to the connectors connecting the control and power PCB together
- The outer top and bottom layers should only have local signal routing, especially the bottom layer, to ensure good noise immunity
- Internal layers will be 3 signal layers and one layer reserved for power planes

Since the power PCB was routed prior to the any routing being done on the control PCB, the pin headers connecting the two cards together could be placed on the bottom side and locked in position first on the control PCB. The remaining routing was done with these headers as a first premise.

The small pnp/npn drivers stages were placed and routed directly on the top side of the pin headers connecting to the power PCB. Special care was taken to minimize the trace length from the pnp/npn transistors to the pin header on the bottom side of the PCB. After this initial placement and routing was done, the DSP and the power regulators were placed along side one of the edges of the board. The current sensors were placed as tightly as possible together in the middle of the PCB. The component placement can be seen in figure 13.

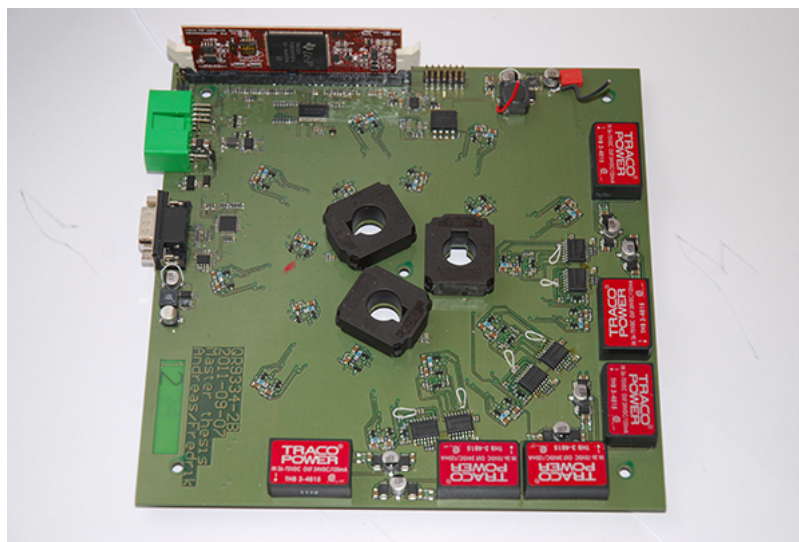


Figure 13: The finished populated controller PCB

When the signals connecting the small pnp/npn driver stages to the gate drivers were routed, a first try to implement so called X-Y routing was made.

X-Y routing means that designated layers are used for routing strictly in X or Y direction of the PCB only, and is used to minimize EMI problems.

However, it became apparent due to the layout of the pin headers, i.e. the ring-shape and the order of the phases as described earlier, made this routing style very inconvenient. Therefore a solution based on the ring shape used on the power PCB was used where open rings with all the 6 signals/isolated power lines were routed in parallel and the different phases were stacked on individual layers in the PCB. These rings can clearly be seen in the composite drawing of the control PCB in appendix A. The rings were orientated to leave the opening facing the DSP and the level shifter so the signal traces from the current sensors could be routed.

The gate driver circuits were placed on the opposite side of the circle opening to equalize the trace length to the small driver stages. The Traco power modules were placed last and were merely placed along side the edges of the PCB that were closest to the gate drivers. A composite drawing of the routing on the different layers can be found in appendix A.

## 8 Building and integrating a powertrain on a Go-Kart

This section will present all the mechanical parts.



Figure 14: Picture showing the complete driveline with the inverter

### 8.1 Cooling

The estimated amount of power that is generated by the inverter in form of heat is calculated according to equation 19. In this fairly rough calculation the switching losses are neglected, since they are small by comparison, and a worst case with 300A flowing out of one phase and 150A in to the two other phases. It is also assumed that the transistors are operating at 175°C and thus have a  $R_{ch} = 5.4m\Omega$ .

$$P_{resistive} = 3 \times (5.4 \times 10^{-3} \times 100^2) + 6 \times (5.4 \times 10^{-3} \times 50^2) \simeq 250W \quad (19)$$

Since this is a prototype there was no need for cost optimizations and such, so it was decided to take a safe route and go with an assumption that the cooling solution needed to be able to handle roughly 1kW. To achieve this and not have the inverter overheat the system is cooled by a heat sink and for additional cooling a fan is used.

### 8.1.1 Heat sink

Since the PCBs are 200x200mm, the heat sink needed to be at least of the same size. The height was determined by efficiency, a taller heat sink would be better to dissipate more heat.

height:	efficiency:
25mm	0.65°C/W
40mm	0.34°C/W

Table 8: 200x200mm Heat Sinks from Farnell AB

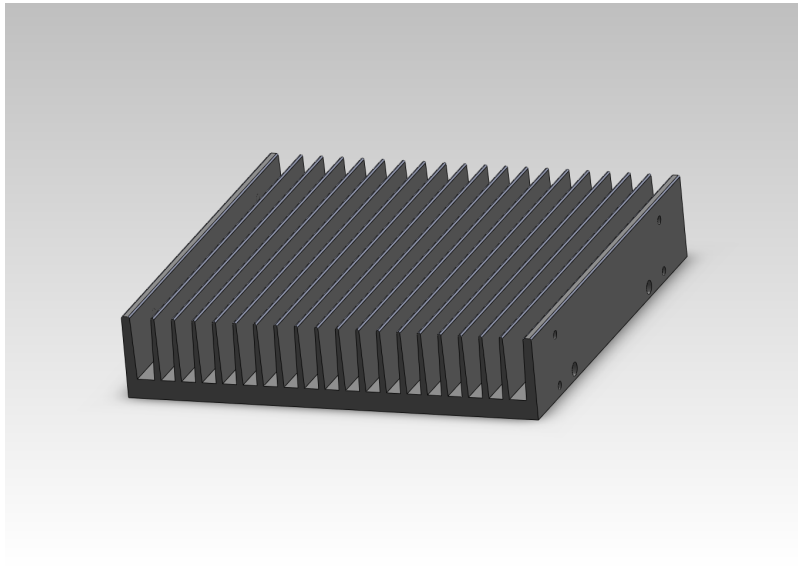


Figure 15: SolidWorks model of a 200x200x40mm heat sink

### 8.1.2 Fan

Because of the data in table above and the estimated power dissipation from the inverter, the 40mm heat sink would be around 340°C higher than the surrounding air. This would require for a fan to be used.

The fan that was supposed to be selected, needed to work in a robust environment where it would be exposed to dirt and rain. With these needs in mind a selection process to find a suitable candidate took place and the conclusion to use a fan for cars was tested, but it was hard to find one that size requirements. However a fan for ATVs was found and purchased and a picture of it can be seen in figure 16.



Figure 16: A picture of the fan.

A mount to fit the fan to the heat sink was required, so one was designed and fabricated. See figure 17.

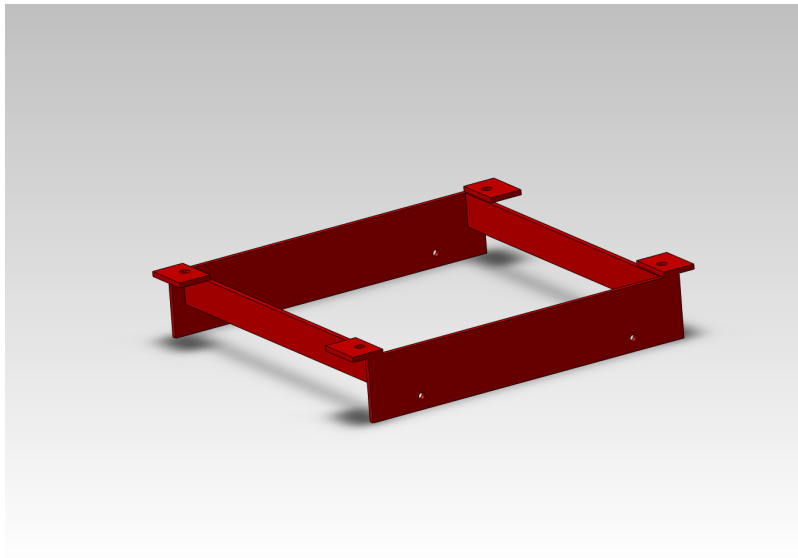


Figure 17: A 3d model of the fan mount

The fan mounted on the heat-sink can be seen in figure 18.

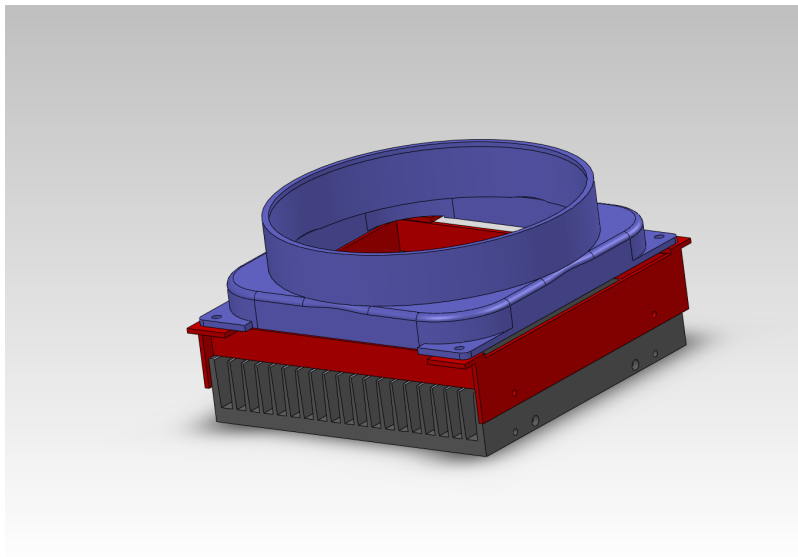


Figure 18: A 3D model of the fan mounted on the heat sink.

## 8.2 Encasing

The PCBs are supposed to be mounted directly on the heat sink, so the encasing would work as a surrounding shell with cut through holes for external connections.

## 8.3 Batteries / Charging

Since this project is a remake of an old project the battery-system from the previous project is kept and is presented below.

### Batteries

Battery pack of 4x 12volt lead batteries of 18Ah each

### Charging

The system is charged by a DC Power Supply

## 8.4 Resolver

A brushless resolver is a type of rotary electrical transformer used for measuring degrees of rotation. It is considered an analog device, and has a digital counterpart, the pulse encoder. The resolver can be compared to an electric motor since it has three windings, a stator and a rotor. Though it is configured a bit differently with one primary exciter winding  $R_x$  and two

secondary windings  $S_x$ , see figure 19. These windings are all located in the stator and the rotor is the core of the transformer. The secondary windings are configured at a  $90^\circ$  angle to each other.

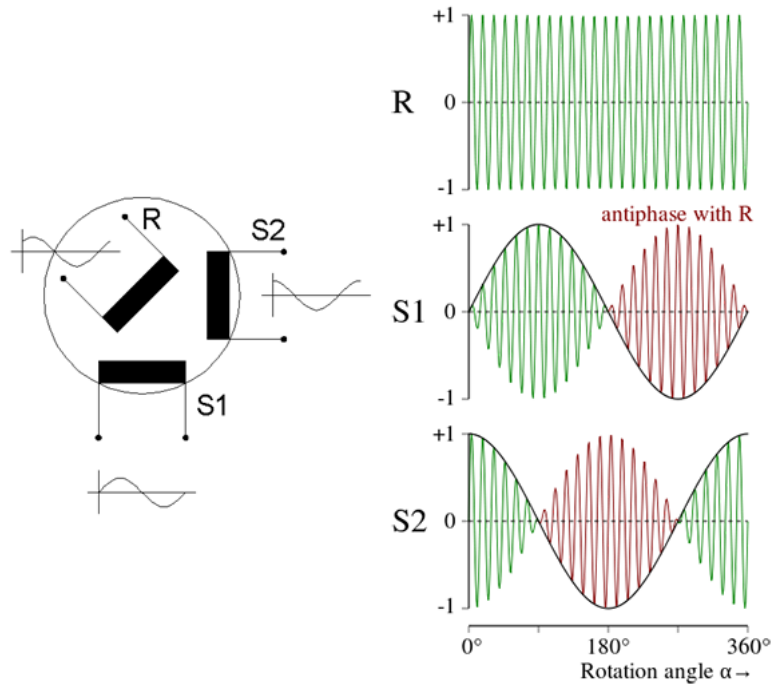


Figure 19: Basic drawing of a resolver and its input/output signal relations [16][17].

The primary winding is driven by a 10kHz sinusoidal current, and this induces currents in the secondary windings via the core. When the rotor is turned the magnetic coupling between the primary and the two secondary windings is changed, and this gives rise to varying amplitudes in the signals read from the secondary windings. This together with the  $90^\circ$  angle between the secondary windings generates output signals in the form of amplitude modulated sine and cosine waves, see figure 19. The specific resolver used for this project has four poles just like the motor used. This means that for every full mechanical revolution the rotor makes, the output signals will contain four periods of the amplitude modulation. It also means that the output signals from the resolver will correspond to the electrical revolutions rather than the mechanical ones.

### 8.4.1 Resolver-to-Digital Converter

Different techniques is used to get a digital representation of the analog data from the resolver, the basic theory of a Resolver-to-Digital Converter is as follows:

- Sample the sine and cosine signal with an ADC.
- Take the arctan function of the sampled sine and cosine signal.

However this is often not good enough due to electric interference, as a solution, a filter is commonly added before the arctan function[18]. An Angle Tracking Observer is one solution, but it is not used in this project. The solution used in this project can be found in section 6.2.

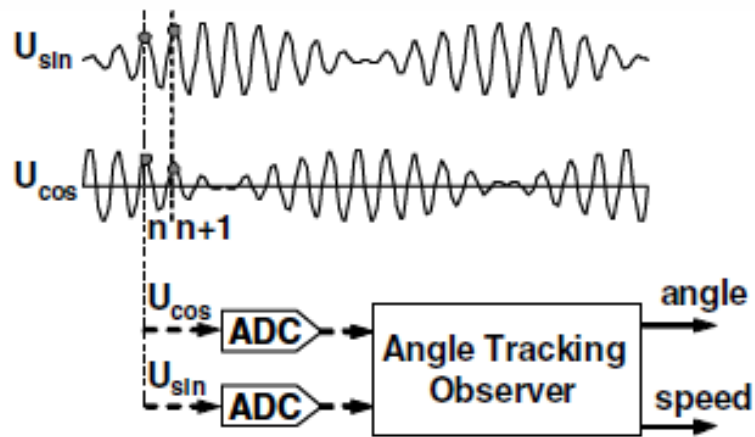


Figure 20: Use of the Angle Tracking Observer for Extracting the Angle and Speed [19]

### 8.4.2 Resolver Mount

To be able to mount the resolver to the motor a custom resolver mount were fabricated.

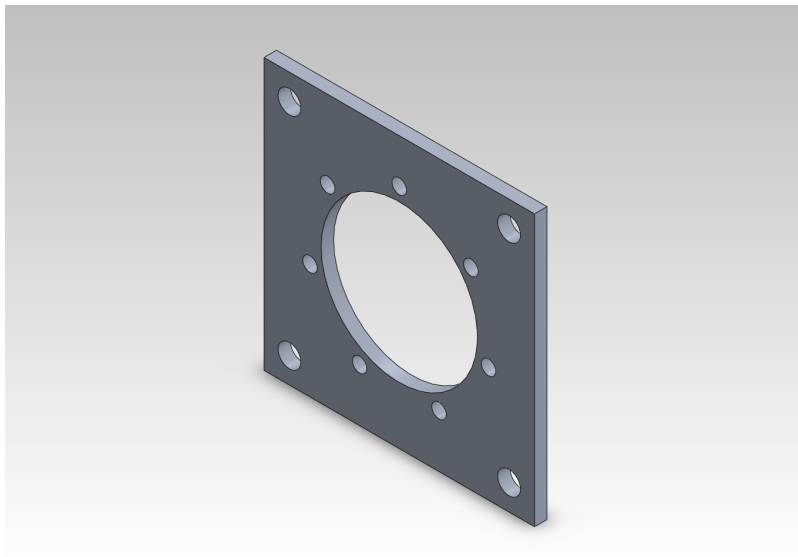


Figure 21: SolidWorks model of the resolver mount

**Resolver Shield** For the resolver to be protected from stone chips and dirt a shield was fabricated.

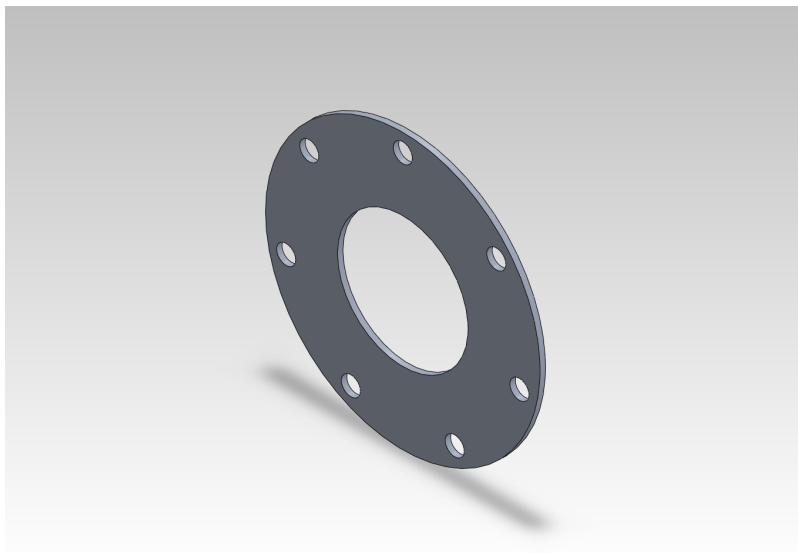


Figure 22: SolidWorks model of the resolver shield

**Resolver Rotor** The rotor bought to the resolver needs an adapter to fit around the motors drive shaft. This was fabricated and it also needed some spacers so that the rotor could be fixed between two washers.

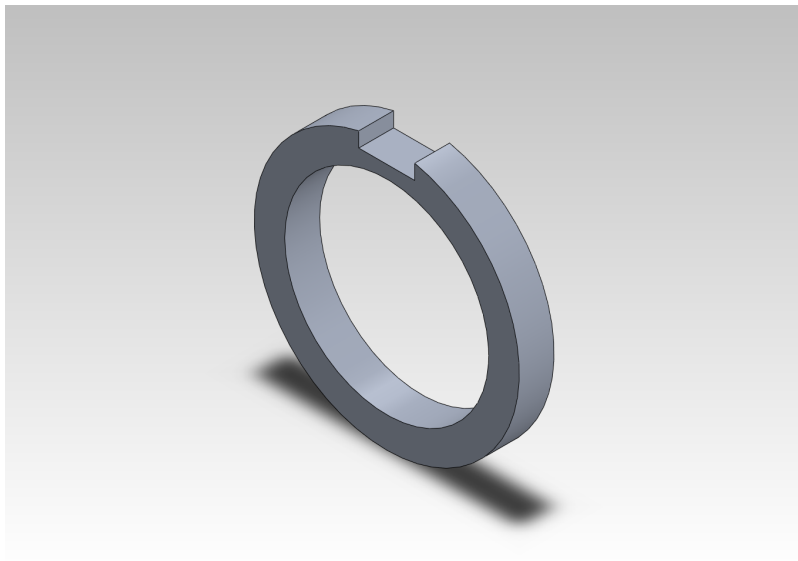


Figure 23: SolidWorks model of the resolver rotor adapter

## 8.5 Drive line

Since this project is remake of an old project the drive line is kept and is presented below, see figure 24 for a picture of the complete drive line on the go-kart.

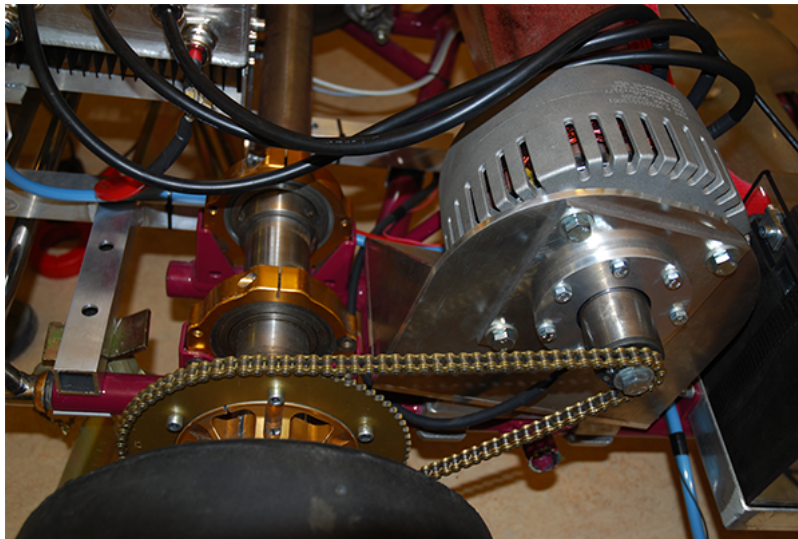


Figure 24: Picture of the driveline

### Drive sprocket

The engine axle is not of a go-kart-standard an adapter is used to drive a drive sprocket. The drive-sprocket used has 13 teeth.

#### **Driven sprocket**

The driven sprocket is of a standard go-kart size and has 70 teeth.

#### **Roller chain**

The roller chain is a go-kart chain

### **8.6 Engine mount**

The old version of the go-kart that this project is upgrading had an existing engine mount. The problem with the old one is that it there were not really any space to fit the resolver. This resulted in that a new engine mount was designed and fabricated, together with the resolver mount.

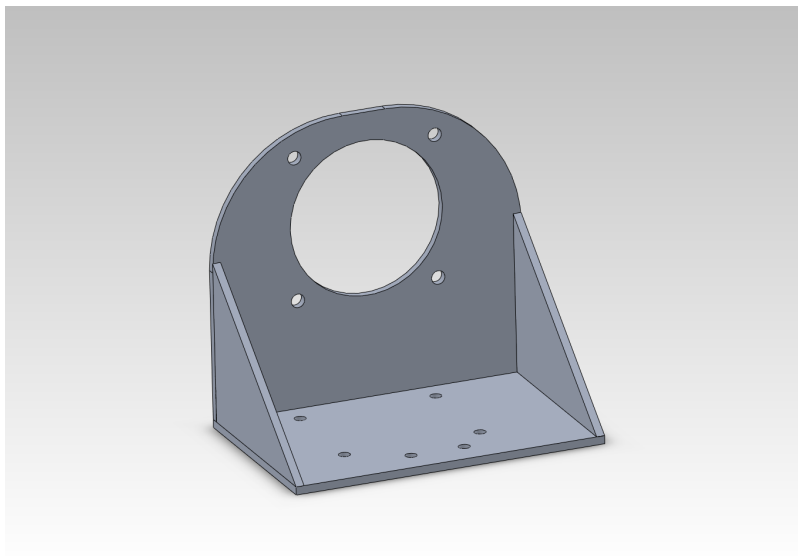


Figure 25: SolidWorks model of the engine mount

### **8.7 Inverter mount**

To be able to mount the inverter with the heat sink and the fan on the go-kart, a custom mount was fabricated. The idea is to mount it at the back of the go-kart, behind the rear axle. The mount is attached to the go-kart chassis at 3 points, 2 are to the left and right just behind the axle and 1 point between the axle and the seat. An extra requirement is that it should be easy to remove or attach the assembled inverter, this lead to a solution where the assembled inverter is attached over the chassis, the drawback of

this is that the assembled inverter would have an unnecessarily big space under it. The mount can be seen in figure 26.

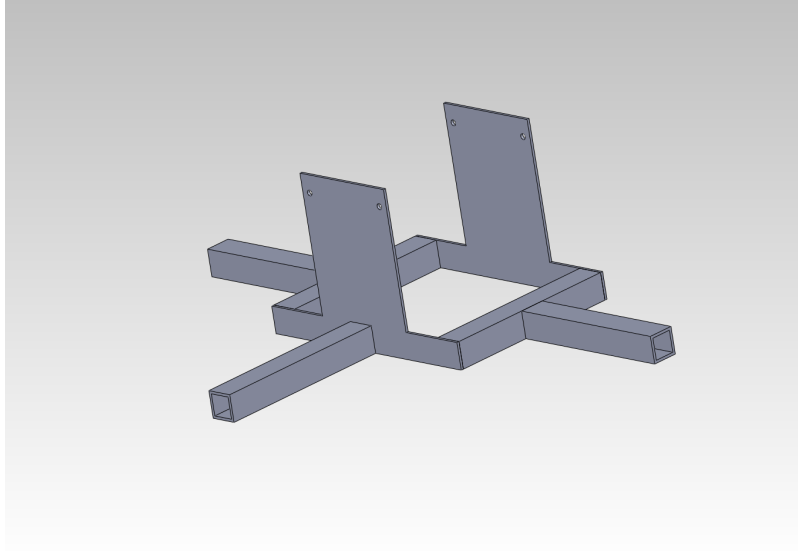


Figure 26: SolidWorks model of the inverter mount

## 8.8 Front panel

The front panel is where the driver can interact with the control system and turn on/off power to the complete system. It consists of a pre-charge switch to charge the capacitors, an on/off power switch, 2 flip switches with 1 blue LED respectively to see on/off and also 1 red and 1 green LED. The panel can be seen in figure 27.



Figure 27: Picture taken of the front panel

## 9 Verification and testing

### 9.1 Software

Since the DSP (TMS320F2833x) offers real-time analysis, more on this in section 6.1, software verification can be carried out live on the DSP, this has been done both on a evaluation board and on the custom designed control board for this project. Details on the software verification will follow in the sections below.

A lot of the software verification was done in multiple steps on different circuit boards to be able to verify in parallel with the design of the projects own circuit board and finally on that board. All tests that were carried out on the old inverter were also done on the new inverter built in the project and the verification produced positive test results in all cases.

#### 9.1.1 Verification of Current Measurement Calibration

The calibration was done just by starting up the system and checking so that the offset calibrated would represent 1.5 volt on all systems.

#### 9.1.2 Verification of Current Measurement

##### Development board

The current measurement have been verified using a potentiometer in the range 0.0 to 3.0 volt connected to the current measurement pins. The measured value in the DSP was then compared with a multimeter.

##### First step with an old inverter

In a first try to verify the current measurement, 3 wires were put through a LEM-sensor and was short circuited so that they would run 3.0A each. The software reading ranged between 8.5 to 9.0A. The 0.5A were considered an acceptable margin when discussed with QRTECH.

#### 9.1.3 Verification of Accelerator reference

##### Development board

The acceleration reference have been verified using a potentiometer in the range 0.0 to 3.0 volt connected to the current measurement pins. The measured value in the DSP was then compared with a multimeter.

##### First step with an old inverter

In a first try to verify the measurement of accelerator reference, two

potentiometers in the range 0.0 to 3.0 volt were connected to the controller PCB extension port. Then the result in the DSP was compared with a multimeter.

#### **9.1.4 Verification of Fan control and temp measurement**

##### **Development board**

The fan control have been verified using a potentiometer in the range 0.0 to 3.0 volt connected to the temperature measurement pin. The measured value in the DSP was then compared with table 5.

##### **First step with an old inverter**

The same tests as above were carried out on the development-board.

##### **With a motor and the project's inverter**

The same tests as above were carried out on the old-inverter but the fan was also attached.

#### **9.1.5 Verification of interrupt duty cycle**

The time the DSP needs to execute an interrupt is not allowed to exceed the period time that interrupt. The interrupt in question is the 40kHz interrupt that controls the SVM generation algorithm. The length in time of the interrupt was measured by setting a pin high when the interrupt started and pulling it low when it ended and then the time was measured with an oscilloscope to see if it was under 100% of the period time of the interrupt. The test showed that the marginal is around 30% when running interrupts at 40kHz.

#### **9.1.6 Verification of switching ADC-channels**

Since the system is changing which ADC-channels to sample during runtime, it was verified so that the right channels were sampled at the right time and would not interfere with each other. This was done by using different input on the different ADC-channels that might interfere with each other and looking at the sampled data during runtime to see if there were fluctuations that shouldn't be there.

#### **9.1.7 Verification of the Driver Disable**

The driver disable was verified with the hardware produced in this project, the testing were done so that the pin was toggled during a run of the system

and then the drivers output were looked at through an oscilloscope.

### 9.1.8 Verification of the Speed Measurement

The verification of the software was done so that during a run with the inverter and a spinning motor, a fixed revolving speed was used to create an angular velocity and then using the primitive function to get the angle as an input to the speed calculations made in the software. The results were also compared with the data provided by the resolver and the QEP-module to see so that they wouldn't deviate too much from each other.

## 9.2 Hardware

This section will describe and discuss the testing process of the hardware. Measurements done on the hardware will be discussed and the procedures for testing the hardware will also be discussed.

As the hardware was assembled and ready for the first test runs, some first power up tests were done. At first the power was just connected to the control PCB and the different voltages on the card were measured. At this stage a first problem was encountered, one of the Traco-modules did not output the correct voltage. An inspection with an IR-camera was then done to look for malfunctioning components. An OP-amp in the voltage feedback from the isolated power connected to the Traco-module in question proved to develop a lot of heat. Since this feedback was from the original design where the isolated power was controlled by the DSP, the OP-amp was simply removed and the problem thus solved. After the initial power up test connectivity to the DSP via the JTAG interface was established.

At the first test run in the lab with the motor, a decision was made to do the test run without the capacitors on the power rings on the power PCB. This was done to enable a comparison between the measurements with and without the capacitors. The snubbers on the MOSFETs were not mounted at this stage either. A current limit of about 10A was used on the power supply to limit the current in case of breakdown. However, this combination proved catastrophic. As the motor made a few first turns, the lack of input capacitance made power supply hit the current limit and then a kind of oscillation between the inverter and the power supply occurred. This led to large voltage spikes that eventually led to a catastrophic failure of the 5V regulator and the DSP on the controller PCB.

After this first failure the first version of the snubbers were mounted to suppress the overshoot and the ringing. The noise created by these oscillations were picked up by the control card and caused a lot of problems. In picture

28 the induced oscillations on the 5V supply are clearly visible, at the time of the measurement, the switching of the half bridges were on but no current was output. With larger currents, the ringings became larger in amplitude.

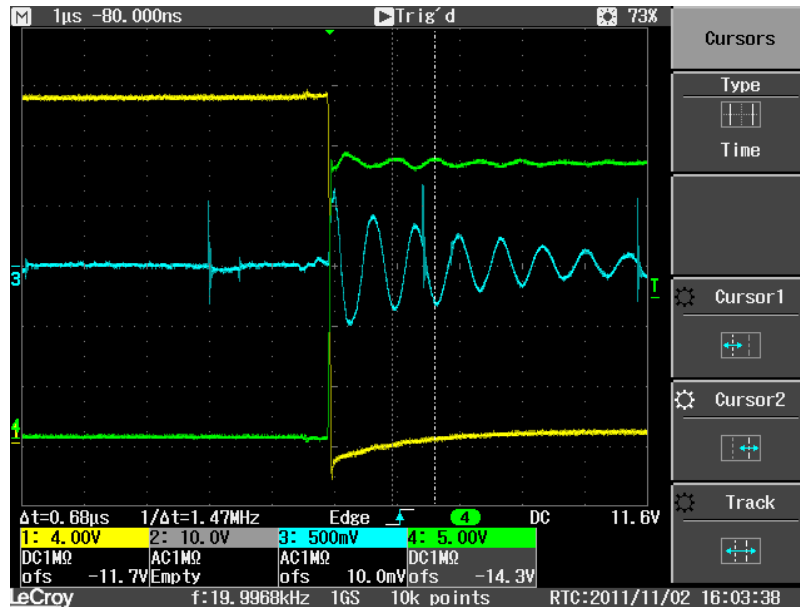


Figure 28: Induced oscillations on 5V supply. Ch1: Source-Drain on upper MOSFET, Ch4: Source-Drain on lower MOSFET and CH3: 5V supply line.

This noise seen on the 5V was also present on the 3.3V supply, since it is derived from the 5V supply, although it were somewhat suppressed.

The resolver with surrounding circuitry showed some severe impact of this noise as well, though when measured it didn't seem as it came from the controller PCB, so it was assumed that it was picked up in the cable connecting the resolver to the PCB. More importantly, it caused a lot of problems on the feedback signals from the resolver. At every flank of the switching a spike was induced on the signals from the resolver. To suppress this a shield was added to the cable and a lot of tuning of the filter on the resolver signals were done. The noise caused the encoder output of the R/D converter IC to jitter quite badly, and this in turn lead to the angle tracking circuitry in the DSP to count a step backwards every now and then. The filter was never really able to suppress the noise to a satisfying level though. There were additional problems caused by these ringings where the JTAG device used to communicate with the DSP and the DSP itself sustained damage.

As the snubbers and the reverse recovery capacitors were replaced, the oscillations were suppressed to more acceptable levels, and tests in a rig where a DC-motor and an electronic load was used to load the motor driven by

the inverter. This enabled tests with higher currents. During these tests a final adjusting of the snubbers was done, to the final values described in section 7.3.4. From these tests it became apparent that the noise found on the control PCB were strongly coupled to the galvanic contact with the power PCB through the shared input power from the same power supply. When this was separated almost all of the problems were gone.

These tests in the rig also served to investigate how the input capacitance on the power PCB is most suitable. Tests were done without the capacitors mounted on the power PCB, and with external capacitors. Combinations with a  $10mF$  aluminum capacitor and  $4.7mF$  plastic film capacitors were conducted. These capacitors were connected with short cables to the input terminals on the power PCB. In a test where only the aluminum capacitor was used, ripple currents were measured to exceed  $200A$  to/from the external capacitor. The tests clearly showed that the best choice is to have the capacitance as close to the half bridges as possible, and thus the solution with the capacitors mounted on the copper rings deemed to be the best.

As the input capacitance, snubbers and the reverse recovery capacitors were adjusted to their final values, almost all of the noise picked up by the controller PCB were gone. A presumed problem with the current sensing was also discovered during these test, were the DSP reported very large output currents (in excess  $200A$ ) when the input current were measured in the range of  $5 - 30A$ . This was just assumed to be of lesser importance and not hardware related, so not much attention was given to it at this point.

As the test in the rig were finished, the system was mounted on the actual go-kart and the tests and measurements done in the rig were repeated with the battery supply. In this case the problem with shared input power from the same source could not be solved with actual galvanic separation. Though the problem was solved through the use of long separate cables from the battery to supply the control PCB with input power. As everything seemed to work well, a first test drive was performed. The test drive resulted in an other catastrophic failure, where one of the MOSFETs actually exploded. It was concluded that an avalanche breakthrough had occurred. After repairs, measurements were taken via a small RC-filter on one of the output phases simultaneously as the current was measured. This revealed why the output currents was measured as high as they were. The angle tracking offset was wrong and this lead to the inverter driving the motor as a pure inductance, leading to a phase shift between voltage and current of almost  $90^\circ$ . This was adjusted in the software and everything worked as intended.

## 10 Result

This section presents the result of the project, a summary of how the goals were fulfilled and that the set of demands were satisfied.

The primal goal of this project was to redesign an existing inverter to fit a changed set of demands.

Second to this is that the inverter is to be implemented with a complete driveline on an electric go-kart and the go-kart should be drivable.

### Supply Voltage

The system can work in a DC supply voltage between 36-72 volt, since this is the range of which certain components do work in.

### 3 phase Alternating Current

As can be seen in the choice of transistors, the system should in theory be able to manage 3x 180A per phase during short intervals which is well over the 300 that it was specified for. However this has not been tested with currents over 150A flowing out of the inverter.

### Torque control

Utilize a closed feedback-loop with a pair of torque-setpoints, current-measurement as feedback together with the rotor-angle of the PMSM.

### Cooling

As seen in section 8.1 the system have both an active (fan) and a passive (heat sink) cooling system to prevent the inverter from overheating and possibly sustaining damage.

### Mechanical

As can be seen in section 8 all mechanical parts needed to fit the system on the go-kart have been designed and manufactured.

### CAN

Hardware support for CAN-communication is implemented to enable future development of communication and interactions with the inverter.

### Safety aspects

In section 3, safety aspects in terms of fault-tolerance and robustness have been analyzed and those have also been implemented in the project.

### Angle measurement

The angle feedback from the motor to the control loop should be done by implementation of a resolver and a R/D (Resolver to Digital) Converter IC, prechosen by QRTECH.

## 11 Discussion

In this section ideas for improvements and other solutions that need more investigation are discussed.

### **New batteries**

The batteries used were normal lead-acid batteries which has the benefit that they are really easy to recharge and they have a long survivability. However they can't produce the same amount of current while keeping the power steady as lithium-ion batteries as an example. An other benefit of Lithium-ion batteries is the high energy density compared to lead batteries, i.e. for a given capacity the Li-ion batteries are much lighter then traditional lead acid batteries. Therefore it would have been an improvement to get new batteries. However, a draw back to the lithium-ion batteries is the cost, they are quite expensive.

### **JTAG**

Considering that 4 JTAG-devices were killed during the project, it became apparent that these did not have any safety features built in. Therefore it could be wise to implement some safety features on the JTAG interface. To be on the safe side, the best solution here might be to galvanically isolate this interface with optocouplers or something equivalent. This would ensure that voltage spikes, both positive and negative, would not reach the JTAG-programmer and thus not burn it.

### **CAN-connector**

In a future revision of the hardware, the CAN interface should maybe have a separate connector. Since in this design, it is sharing the connector with all the other interfaces and even the power supply to the control PCB. This made the connector very crowded with all sorts of wiring and for development/prototyping separate connectors for communication would have been preferable.

### **Galvanically separated supply**

As outlined in chapter 9.2 there should maybe have been a solution in place to galvanically separate the entire controller PCB from the power supply of the power PCB. This was briefly discussed during the project, though because of the Traco modules this was not feasible. They need at least 36V to work and the routing on the control PCB would not permit a separation between the 5V regulator which supplies the logic with power and the 6 Traco modules. And to supply the Traco modules as well would mean a quite high demand of power. This means that a "off the shelf"-solution would be too expensive, and to design an own solution would take too long time. So this is indeed a point to take to

the next revision of the hardware.

### **PCB design**

A major item to reconsider in the design choices for the control PCB is the plane connects to the component footprints. In the inverter all copper plane/polygon connects were made without so called thermal reliefs, this made replacing components a nightmare since the copper planes removed all the heat from the solder joints. A small but nice feature to have could have been some indicator LEDs. Maybe a few connected to the DSP and a LED for each supply voltage.

The layer stack-up of the control PCB might need some rethinking as well, since most of the signals routed on the PCB were routed on stacked internal signal layers. In this stack-up there was only one dedicated ground layer, and it was placed in the middle of the stack-up. It has come to our attention that good practice for noise immunity and low radiated noise signals should be routed on a signal layer with a solid ground plane on an adjacent layer. Although the bottom layer were more or less used as a ground shield, with no routing allowed except the absolutely necessary routing to the connectors mounted on the bottom layer. This could maybe have been replaced with an actual metal shield mounted over the power PCB only with holes for the connections to the PCB.

### **TRACO**

In the original design there was a solution for generating the isolated power to the gate drivers and the MOSFETs, by an isolation transformer and some driving transistors controlled by the DSP. This solution could be reworked and suited for the new set of demands. This should be done first and foremost to lower the component cost of the inverter, since the Traco power modules are not cheap. The PCB area required for the isolated power might also be reduced with discrete components rather than the complete modules. However, there is significant work to be done to make a new solution work well, and perform as good as the complete modules. One must also consider that a new switching solution to be controlled by the DSP will naturally demand more of the software and the DSP.

The isolated side of this power supply might also need some rework. Since the isolated power was divided in to +15V, 0V and -8V with a simple series of zener diodes. This was energy wise a very inefficient solution, the IR-camera actually showed that the working temperature of these diodes reached about 70°C. The best solution, but also the most advanced and time consuming, would be a switched transformer with multiple outputs and control circuitry that regulates directly on these outputs.

### Change battery position

As of now, all the batteries are placed on one side which makes the weight very unbalanced, this could be fixed by a change in battery position.

### R/D (Resolver to Digital) Converter IC

The current system have a dedicated IC that is used together with the resolver both for excitation and interpretation. To reduce cost, alternative solutions to this IC is discussed in the following topics: "Resolver excitation" and "Angle Tracking Observer (ATO)"

#### Resolver excitation

The resolver is excited by a 10kHz signal that instead of having the IC constructing it, could be constructed by a PWM from the DSP.

#### Angle Tracking Observer (ATO)

An alternative basic method for interpreting the signals from the resolver in the DSP is to use the inverse tangent method on the sampled sine and cosine modulated output from the resolver, however this is an approach that gives an unfiltered rotor angle and is therefore sensitive to noise [19].

In the Angle Tracking Observer method, a closed-loop state system (state observer) replaces the simple inverse tangent function in order to compute the shaft angle and speed. This is an approach that estimates the rotor angle and having the advantage of rendering a smoother and more accurate rotor angle [19].

An integrator and a PI regulator are connected in series and closed by a feedback loop. A block-diagram of this can be seen in figure 29.

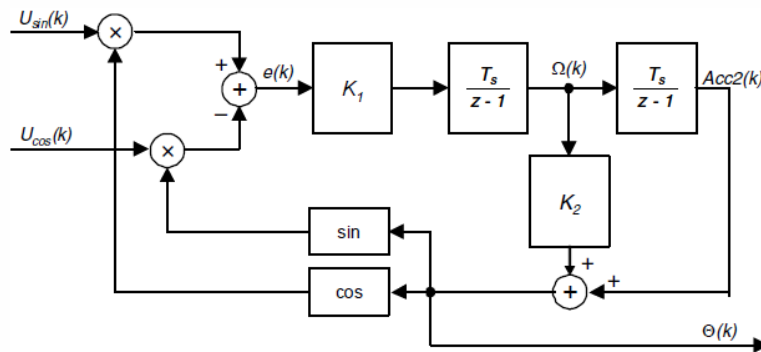


Figure 29: Block Diagram of the Angle Tracking Observer in the Digital Domain [20]

The error is computed as a sine of the difference of the resolver angle  $\alpha$  and the computed angle  $\beta$  as shown in equation 20.

$$\sin(\alpha - \beta) = \sin\alpha \times \cos\beta - \cos\alpha \times \sin\beta \quad (20)$$

For implementation purpose, the sampled resolver outputs are scaled to the range of -1 to 1. After performing this, the Angle Tracking Observer can be implemented as equation 21.

$$\begin{aligned} e_k &= RES_{sin} \times \cos(\Theta_k) - RES_{cos} \times \sin(\Theta_k) \\ \Omega_k &= \Omega_{k-1} + e_k \times K_1 \\ Acc_k &= Acc_{k-1} + \Omega_{k-1} \\ \Theta_{k+1} &= (K_2 \times \Omega_k + Acc_k) \times \pi \\ K_1 &= \frac{T_s^2 \times \omega_n^2}{\pi} \\ K_2 &= \frac{2 \times \zeta}{\omega_n \times T_s} \end{aligned} \quad (21)$$

### **Regenerative Braking**

The hardware is prepared to use regenerative braking but was not implemented in software because it was outside the scope of the project. It would be a good solution to maximize the utilisation of the battery-power since energy would not be wasted as heat during braking.

## 12 Conclusion

The primary goal of the project was, as outlined in section 1.2, to redesign an existing inverter to fit a new set of demands on voltage and current. Although the inverter were not fully tested for the upper limits of the voltage and current demands, the redesign was successful. Thus it must also be concluded that it is not certain that the functionality can be guaranteed at max specified voltage and current. This is simply because testing equipment to test under these conditions were not available. The secondary goal, to implement the inverter in a drive train on a go-kart, was also achieved [21]. The finished inverter is a prototype and there is a lot of optimization of the hardware design, and as stated before, there is still some testing to be done. It can also be said that the lead-batteries were probably not in too good condition, and the go-kart would have more power if they were changed to lithium based batteries. Concerning the project itself, it can be concluded that more time could have been spent on project management, but in hindsight, there seemed to be no time for much more. A very clear conclusion is that more then one prototype should have been built, since much of the testing had to wait for the hardware to be repaired after sustain damage from previous tests.

After the project was finished at QRTECH, we as a group had worked around 200 hours over the budget and we still had around 200 hours left to make the report and presentations done as well. Because of this we feel that since this project were fairly large it would have been good to have an extra set of hands with good knowledge in especially electrical design but also good programming knowledge.

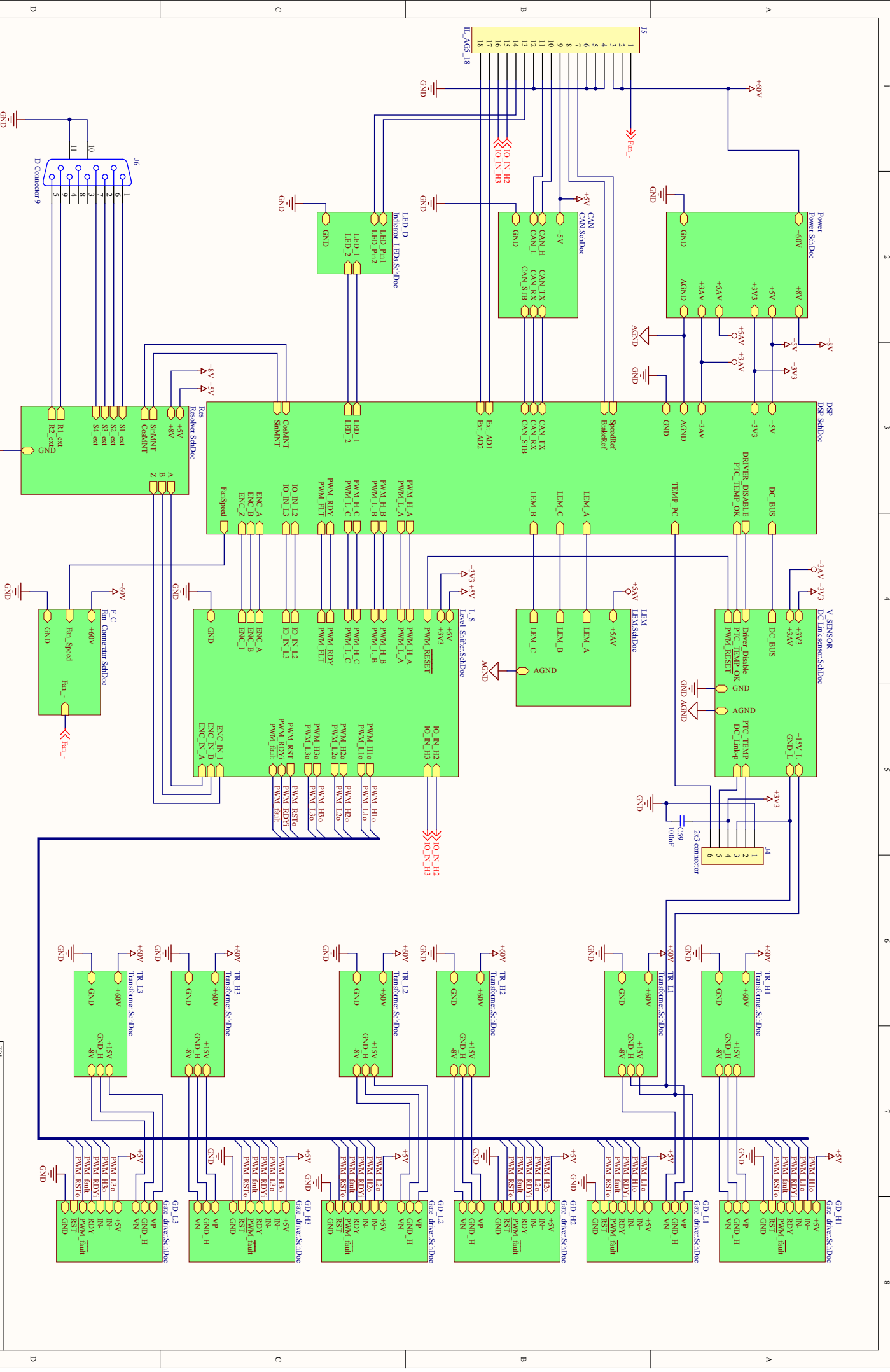
## References

- [1] D. Sperling, D. Gordon, and A. Schwarzenegger, *Two billion cars: driving toward sustainability*. Oxford University Press, USA, 2009.
- [2] European Environment Agency. (2011) Size of the vehicle fleet (term 032). [Online]. Available: [http://www.eea.europa.eu/data-and-maps/indicators/size-of-the-vehicle-fleet/ds\\_resolveuid/284a9269b0b8e08ac5f5ac29f7886460](http://www.eea.europa.eu/data-and-maps/indicators/size-of-the-vehicle-fleet/ds_resolveuid/284a9269b0b8e08ac5f5ac29f7886460)
- [3] United Nations. (2010) World population prospects. [Online]. Available: <http://esa.un.org/wpp/unpp/p2k0data.asp>
- [4] Wikipedia. Can bus. [Online]. Available: [http://en.wikipedia.org/wiki/Controller\\_area\\_network](http://en.wikipedia.org/wiki/Controller_area_network)
- [5] MIT Electric Vehicle Team. (2008) Electric powertrains. [Online]. Available: [http://web.mit.edu/evt/summary\\_powertrains.pdf](http://web.mit.edu/evt/summary_powertrains.pdf)
- [6] D. O. Neacsu. (2001) Space vector modulation, an introduction. [Online]. Available: <http://et.upt.ro/admin/tmpfile/fileM1224954797file490353adde0d4.pdf>
- [7] M. Alaküla, *Power Electronic Control*. KFS, 2003.
- [8] IEA, Lund Institute of Technology, *Power Electronic Control*. KFS, 2003.
- [9] A. Urquizo. (2011) Pid controller overview. [Online]. Available: [http://upload.wikimedia.org/wikipedia/commons/4/43/PID\\_en.svg](http://upload.wikimedia.org/wikipedia/commons/4/43/PID_en.svg)
- [10] B. Thomas, *Modern Reglerteknik*. Liber, 2008.
- [11] Texas Instruments. (2011) Tms320f28335 datasheet1. [Online]. Available: <http://www.ti.com/lit/ds/sprs439m/sprs439m.pdf>
- [12] EPCOS. (2012) Ntc thermistors for temperature measurement. [Online]. Available: [http://www.epcos.com/inf/50/db/ntcsmd\\_11/SMD\\_NTCs\\_NiBarrier\\_Automotive\\_0603.pdf](http://www.epcos.com/inf/50/db/ntcsmd_11/SMD_NTCs_NiBarrier_Automotive_0603.pdf)
- [13] Infineon technologies. 1ed020i12f, gate driver ic datasheet. [Online]. Available: <http://www.infineon.com/dgdl/Datasheet1ED020I12-FV2.1.pdf?folderId=db3a3043132679fb0113346c911c05a4&fileId=db3a30431689f4420116d3baa8120c6c>
- [14] Infineon technologies. Ipb025n10n3 g, mosfet transistor datasheet. [Online]. Available: [http://www.infineon.com/dgdl/IPB025N10N3+G-Re2.03.pdf?folderId=db3a304313b8b5a60113cee8763b02d7&fileId=db3a30431ce5fb52011d1ab1d9d51349&location=en.Products.Discretas\\_\\_Standard\\_Products.MOSFETs.Power\\_MOSFETs](http://www.infineon.com/dgdl/IPB025N10N3+G-Re2.03.pdf?folderId=db3a304313b8b5a60113cee8763b02d7&fileId=db3a30431ce5fb52011d1ab1d9d51349&location=en.Products.Discretas__Standard_Products.MOSFETs.Power_MOSFETs)

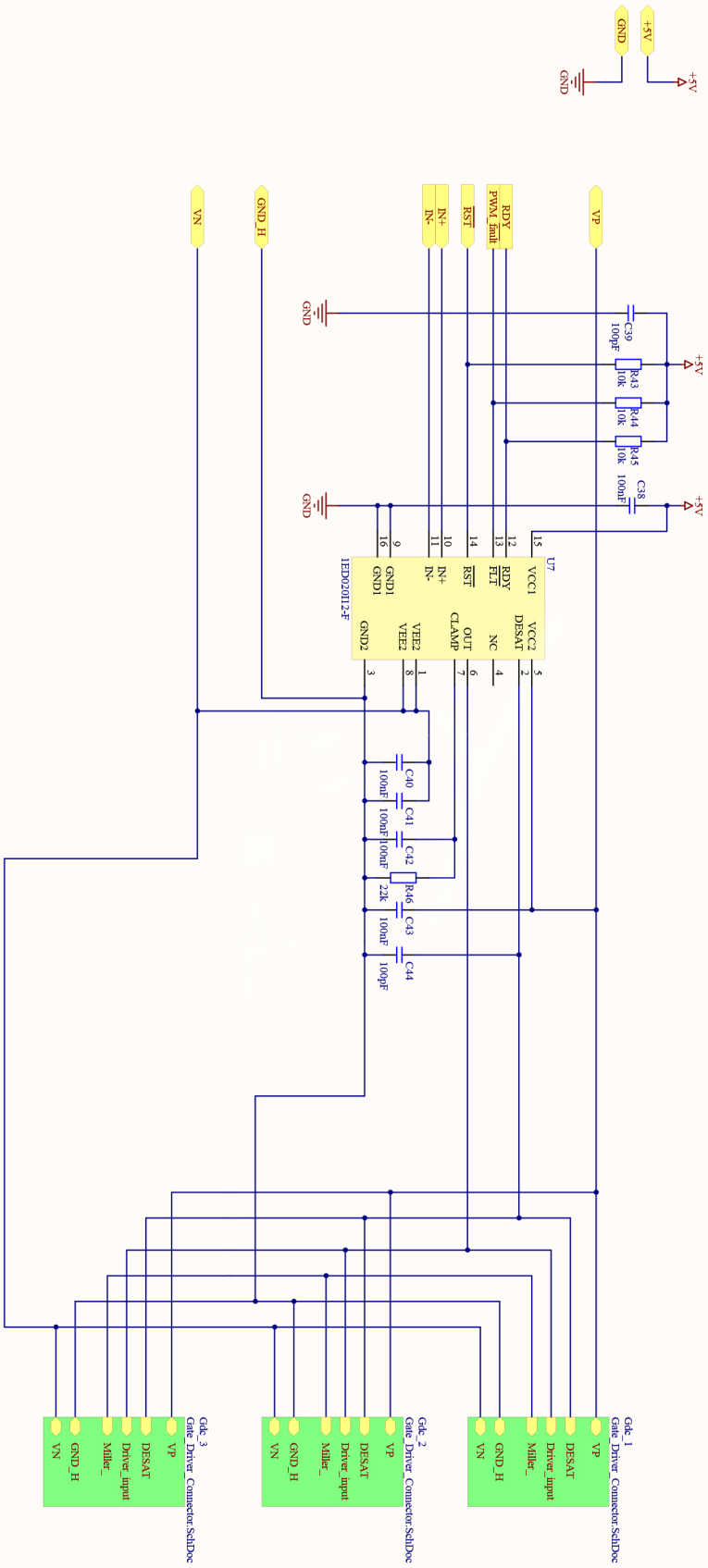
N-Channel\_MOSFETs\_20...250\_.DATASHEET.IPB025N10N3%  
20G\_Re2.03.pdf

- [15] Wikipedia. Thermal resistance. [Online]. Available: [http://en.wikipedia.org/wiki/Thermal\\_resistance](http://en.wikipedia.org/wiki/Thermal_resistance)
- [16] H. Seehagel. (2004) Concept of rotor excited resolver. [Online]. Available: <http://upload.wikimedia.org/wikipedia/commons/6/6d/ResolverPrinzip.png>
- [17] Menner. (2012) Characteristic of a resolver. [Online]. Available: <http://upload.wikimedia.org/wikipedia/commons/9/91/Resolver-Uebertragungsverhalten.svg>
- [18] Admotec Inc., “Tech talk 2: Understanding resolvers and r/d conversion,” 1997. [Online]. Available: <http://www.admotec.com/TT02.pdf>
- [19] Freescale Semiconductor., “56f80x resolver driver and hardware interface,” 2005. [Online]. Available: <http://cache.freescale.com/files/product/doc/AN1942.pdf>
- [20] Freescale Semiconductor, “Using the resolver interface etpu function,” 2009. [Online]. Available: [http://cache.freescale.com/files/microcontrollers/doc/app\\_note/AN3943.pdf](http://cache.freescale.com/files/microcontrollers/doc/app_note/AN3943.pdf)
- [21] F. Lönnblad, A. Öhlund and QRTECH. (2011, Nov.) Electric gokart test dirve. [Online]. Available: <http://www.youtube.com/watch?v=RFh-Bldvg6M&feature=plcp>

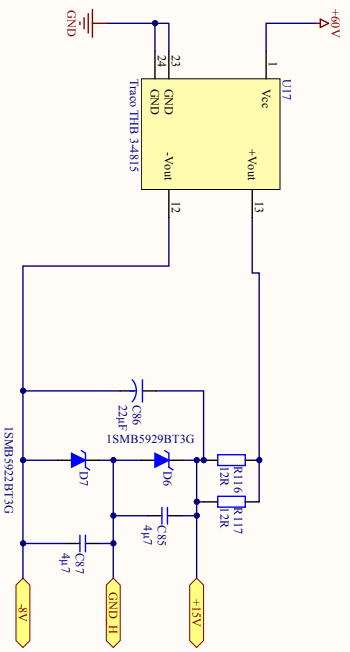
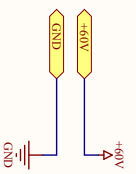
## A Control PCB schematics



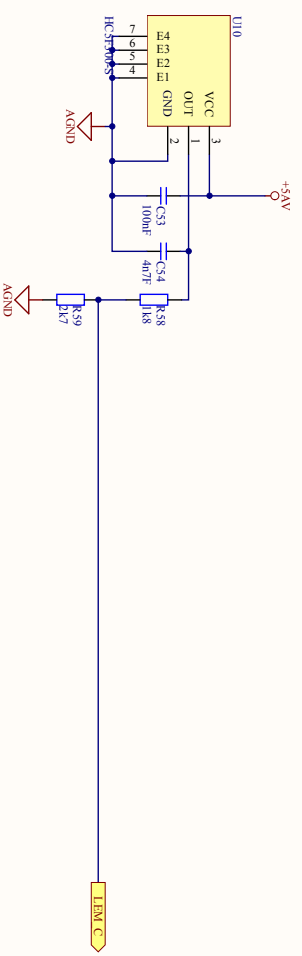
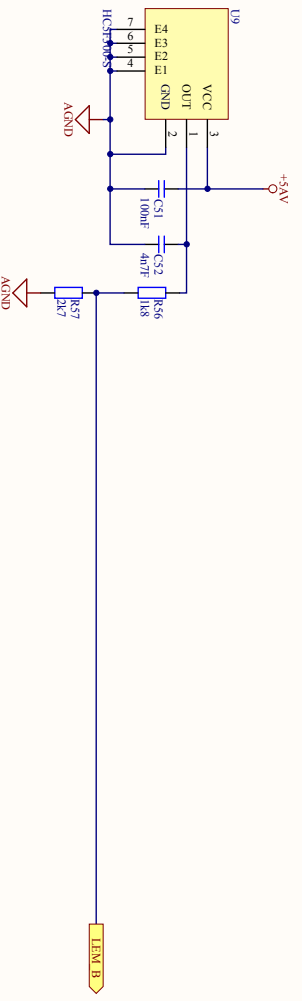
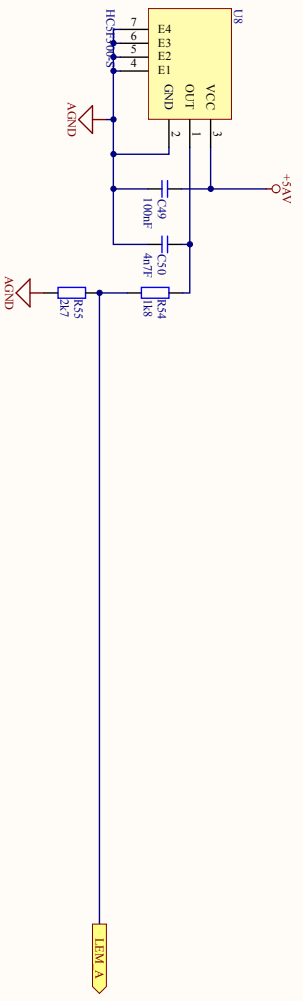
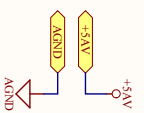
Title	Number	Revision
Size	A3	
Date	2011-12-02	
File	p:0314 Driessystem ElkQuart_Main SchikBhavan By	
Sheet of		



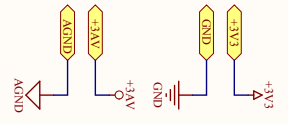
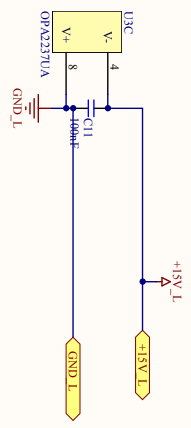
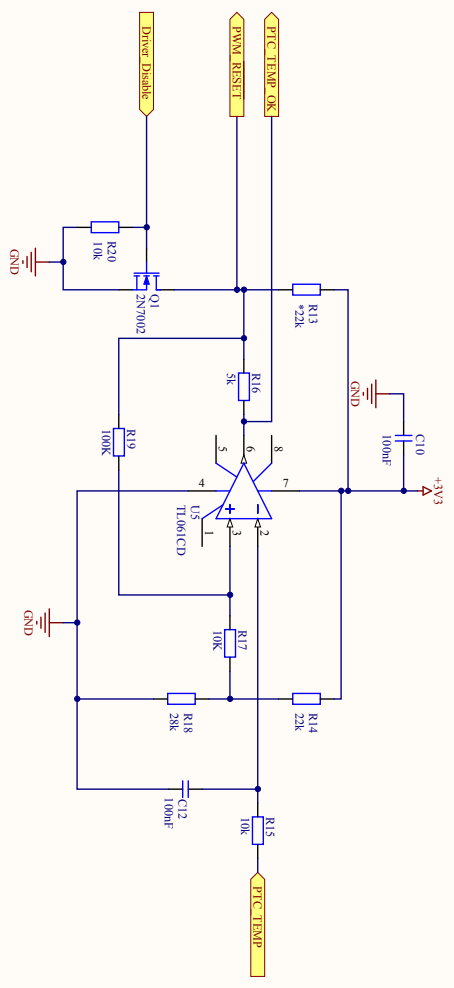
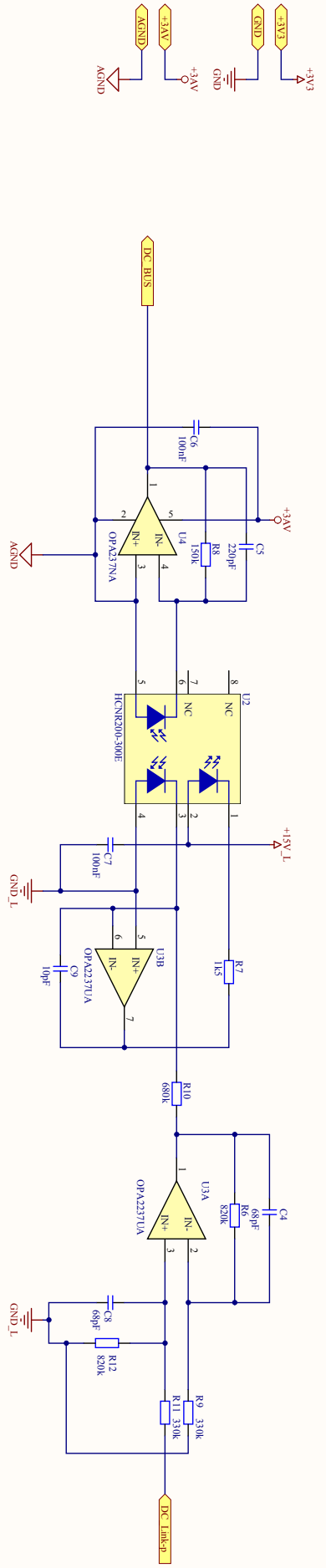
Title		Revision	
Size	Number		
A3			
Date	2011-12-02	Sheet of	
File	P:\9354 Drivsystem ElGokart\Gate_driver	Sheet of	
		File:	



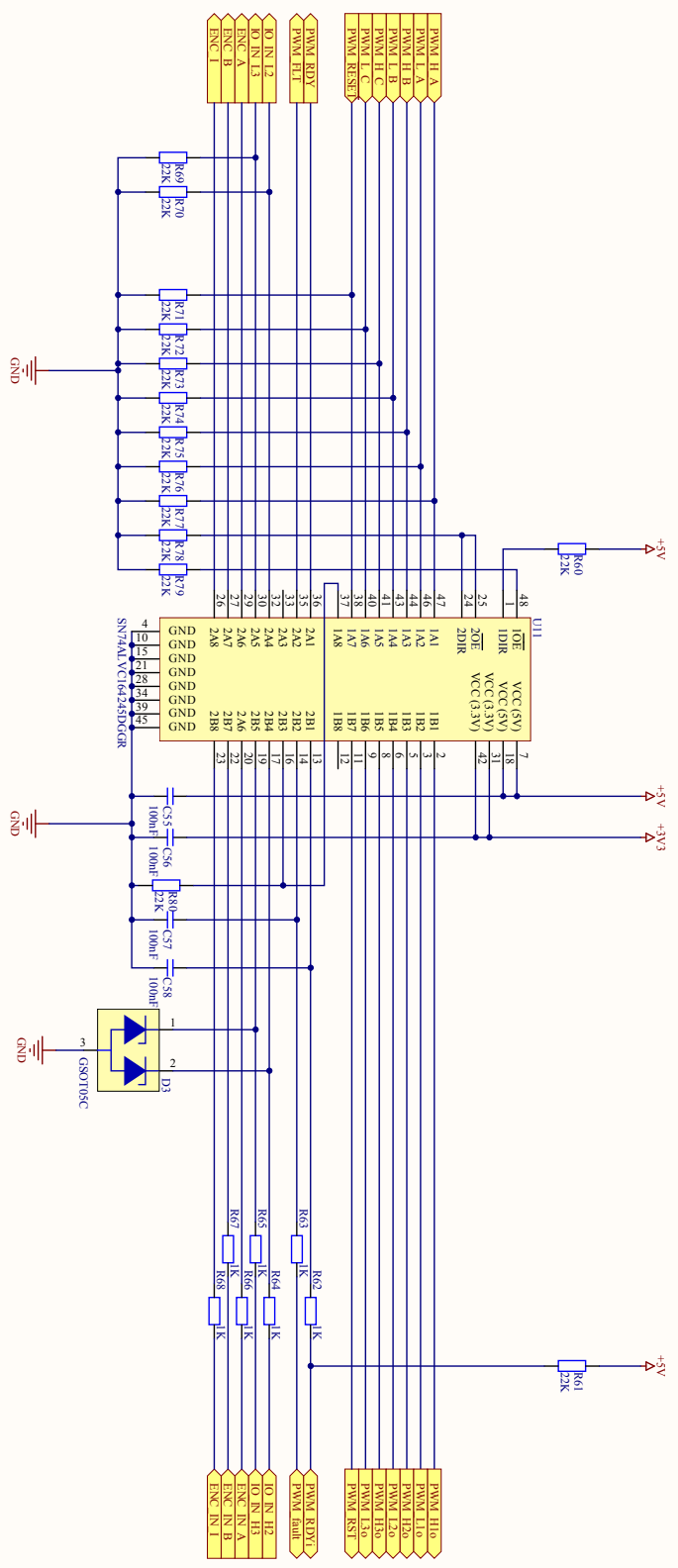
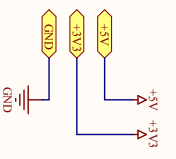
Title		Revision	
Size	Number		
A3			
Date	2011-12-02	Sheet of	
File	P:\9314 Divesystem ElkGard\Transform\9314b3b.v	7	



Title		Revision	
Size	Number		
A3			
Date	2011-12-02	Sheet of	
File	P:\9314 Divisions\EMC\G0404\LEM SCHM\RevB.rvt	8	

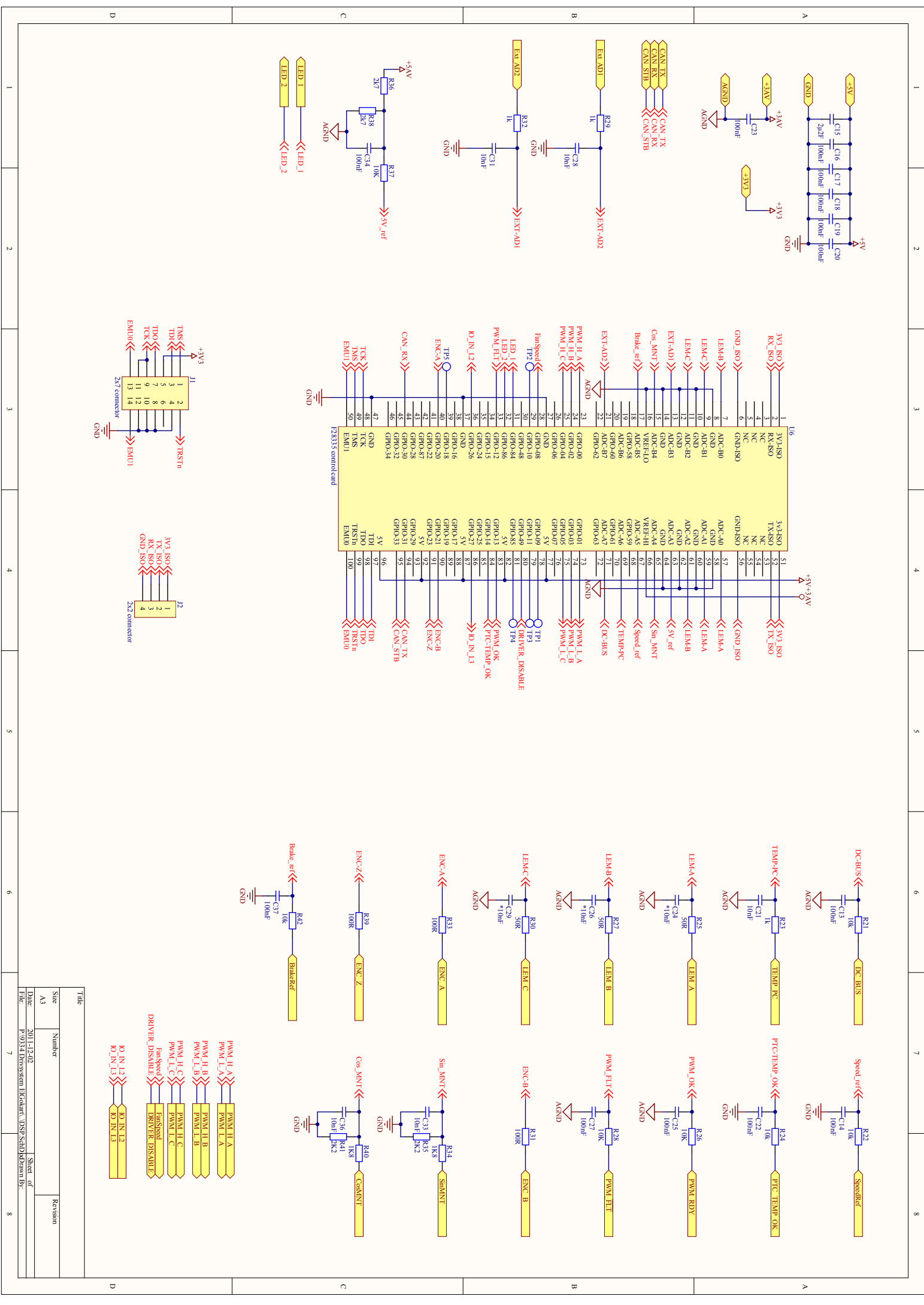


Title		Revision	
Size	A3	Number	
Date	2011-12-02	Sheet of	
File	P:\9314 Drivers\src\Elc\Output\DCLink\src\shimadzu\Bnc		

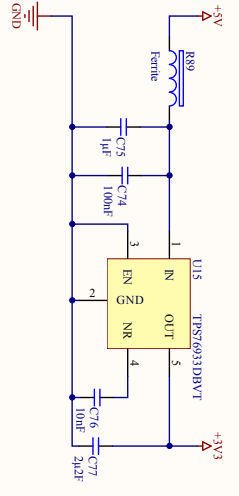
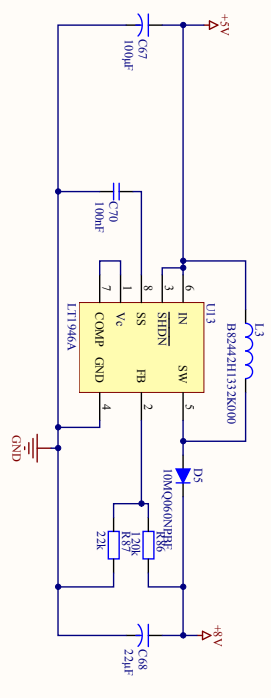
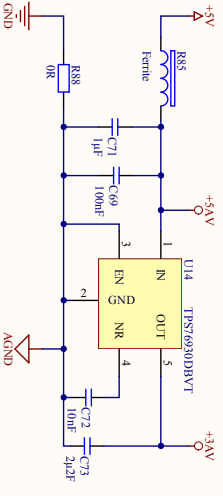
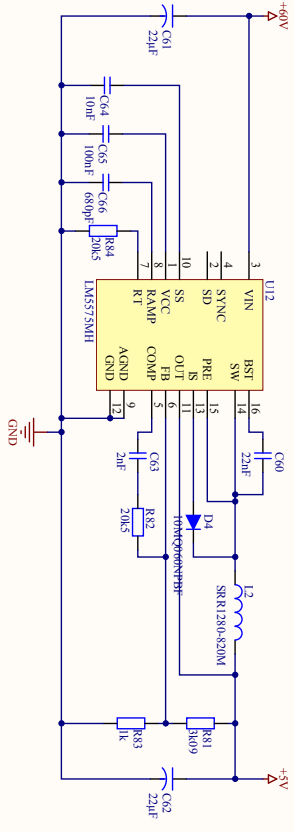
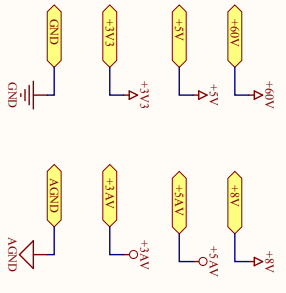


Title		Revision	
Size	Number	Sheet of	Revision
A3			
Date	2011-12-02		
File	P:0314 D:\system\ElGouadi\level Shield\PCB\PCB.kicad_pcb		

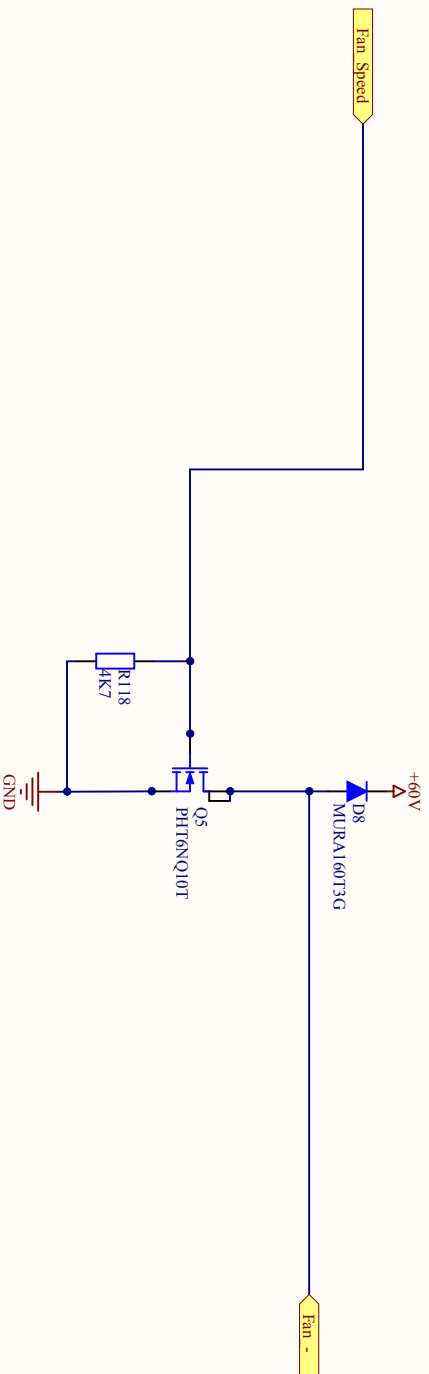
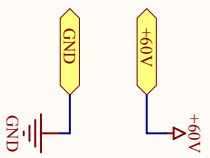




Title	
Size	Number
A3	
Date	Revision
P:0314 D:\Dressen\EMC\Control_VSP_SchB\MD\Drawn By:	
Sheet of	
7	



Title		Revision	
Size	Number		
A3			
Date	2011-12-02	Sheet of	
File	P:\9314_Drvsystem_EIG\Qualif_PowerSch\Drvswrn.Byr	8	

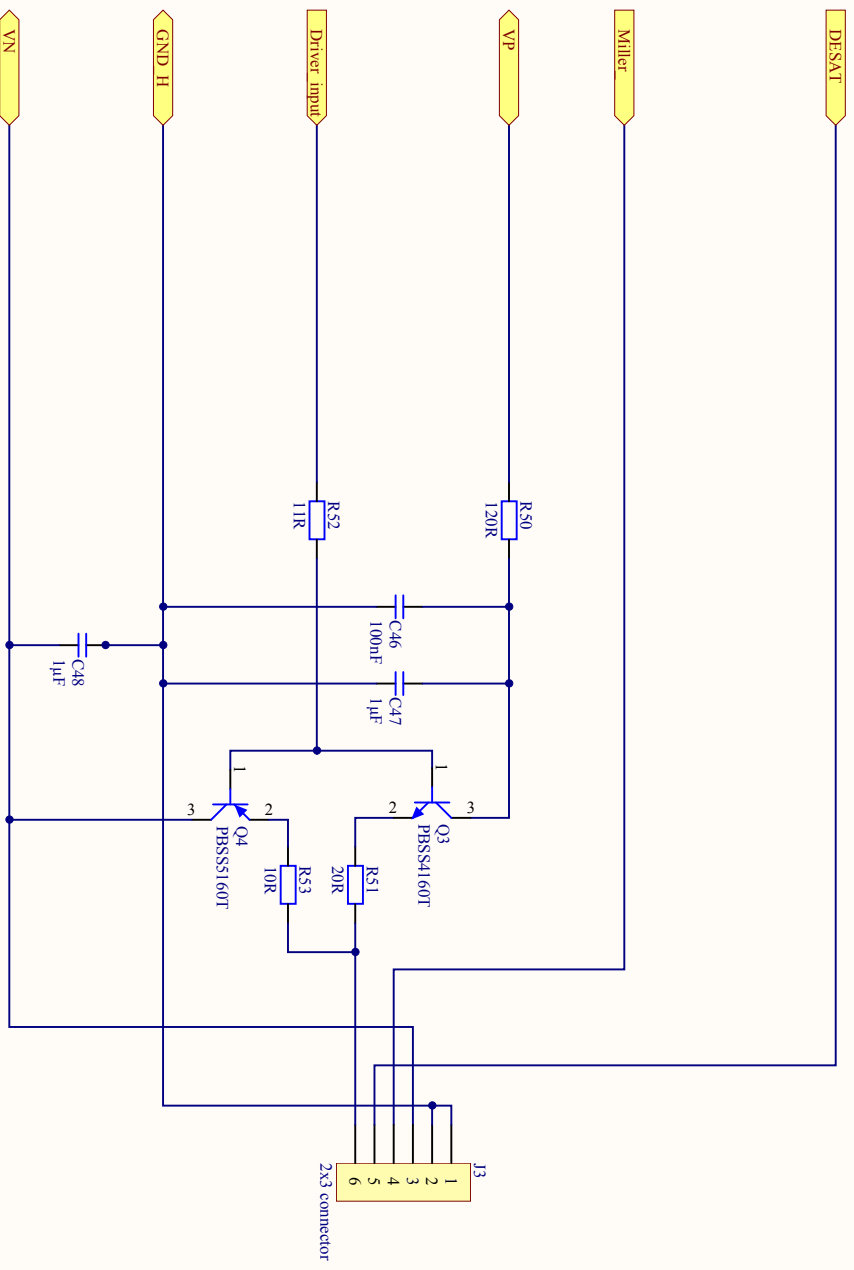


Revision History	
Revision	Change History

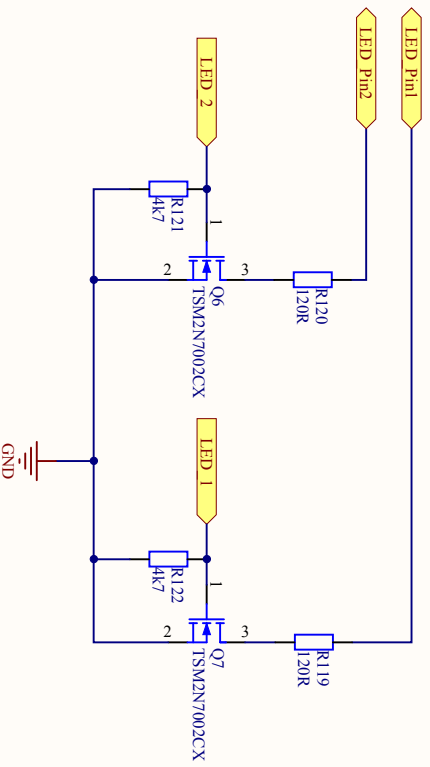
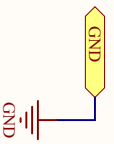
This document is the property of ORTECH and must not be copied, shown to or given to any third party without our written permission.

Title <b>XXXXX - Project</b>		ORTECH AB	
Size: A4	Number:	Megergård 1	SE-412 76
Date: 2011-12-02	Time: 14:16:46	Göteborg	Sweden
File: Fan Connector_SchDoc	Revision: *	Sheet	of





Title		Revision	
Size	Number	Revision	
A4			
Date:	2011-12-02	Sheet of	
File:	P:\9334 Driversystem ElGokart\Gate Driver\Diagram\Bor_SchDoc		



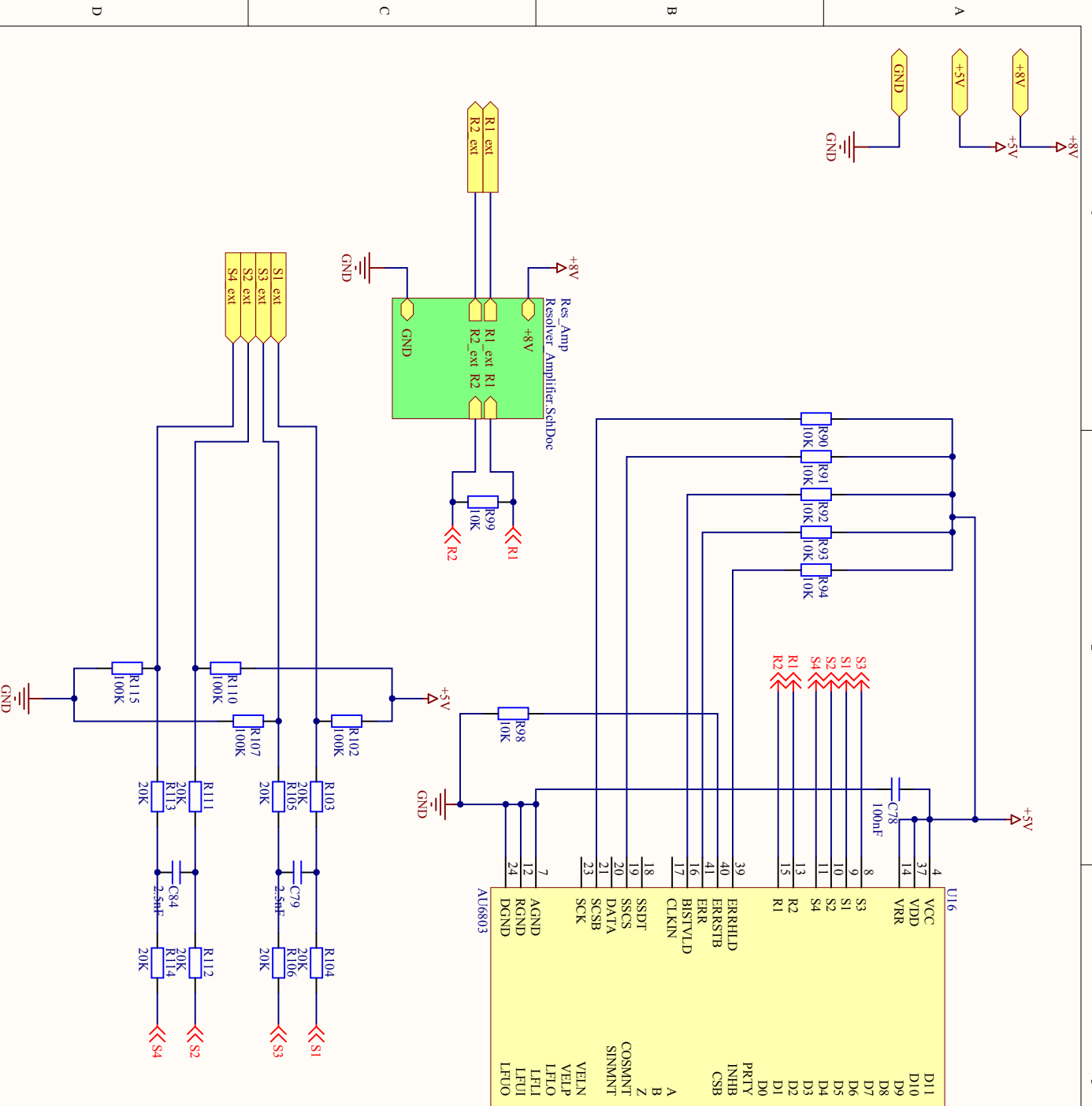
**Revision History**

Revision	Change History

This document is the property of ORTECH and must not be copied, shown to or given to any third party without our written permission.

Title <b>XXXX - Project</b>		ORTECH AB	
Size: A4	Number:	Megenstam 1	
Date: 2011-12-02	Time: 14:16:46	SE-41276	
File: Indicator_LEDs.schDoc	Revision: *	Göteborg	
	Sheet of	Sweden	





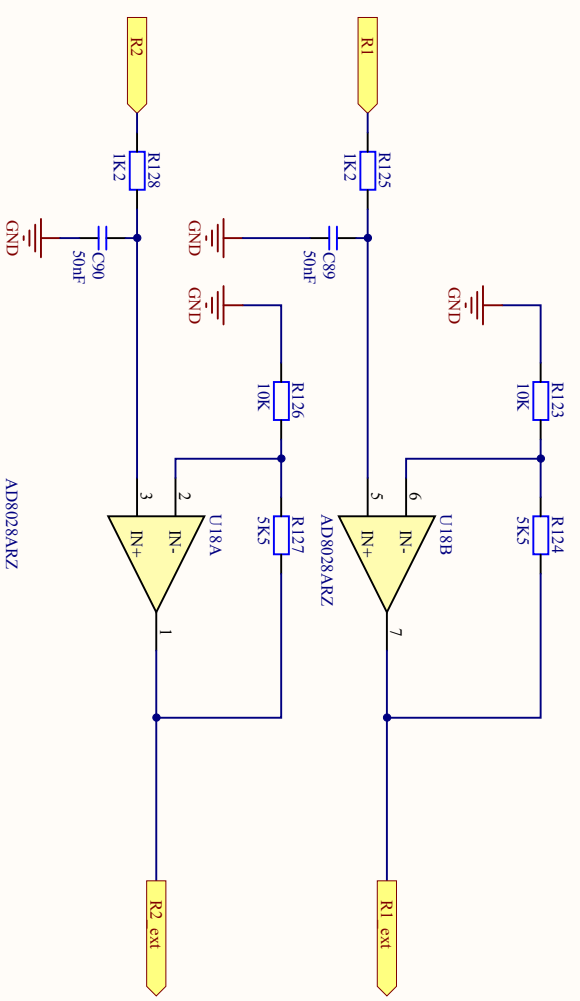
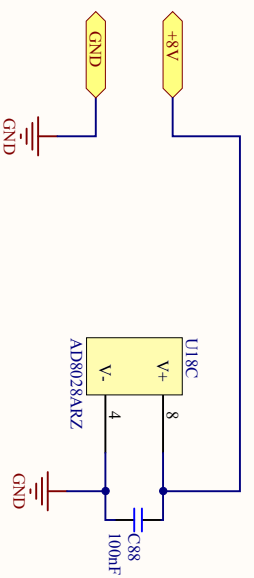
Title		Revision	
Size	A4	Number	
Date:	2011-12-02	Sheet of	
File:	P:\9334 Drivsystem ElGokart\Resolver_SchDoec.dwg	By:	

1

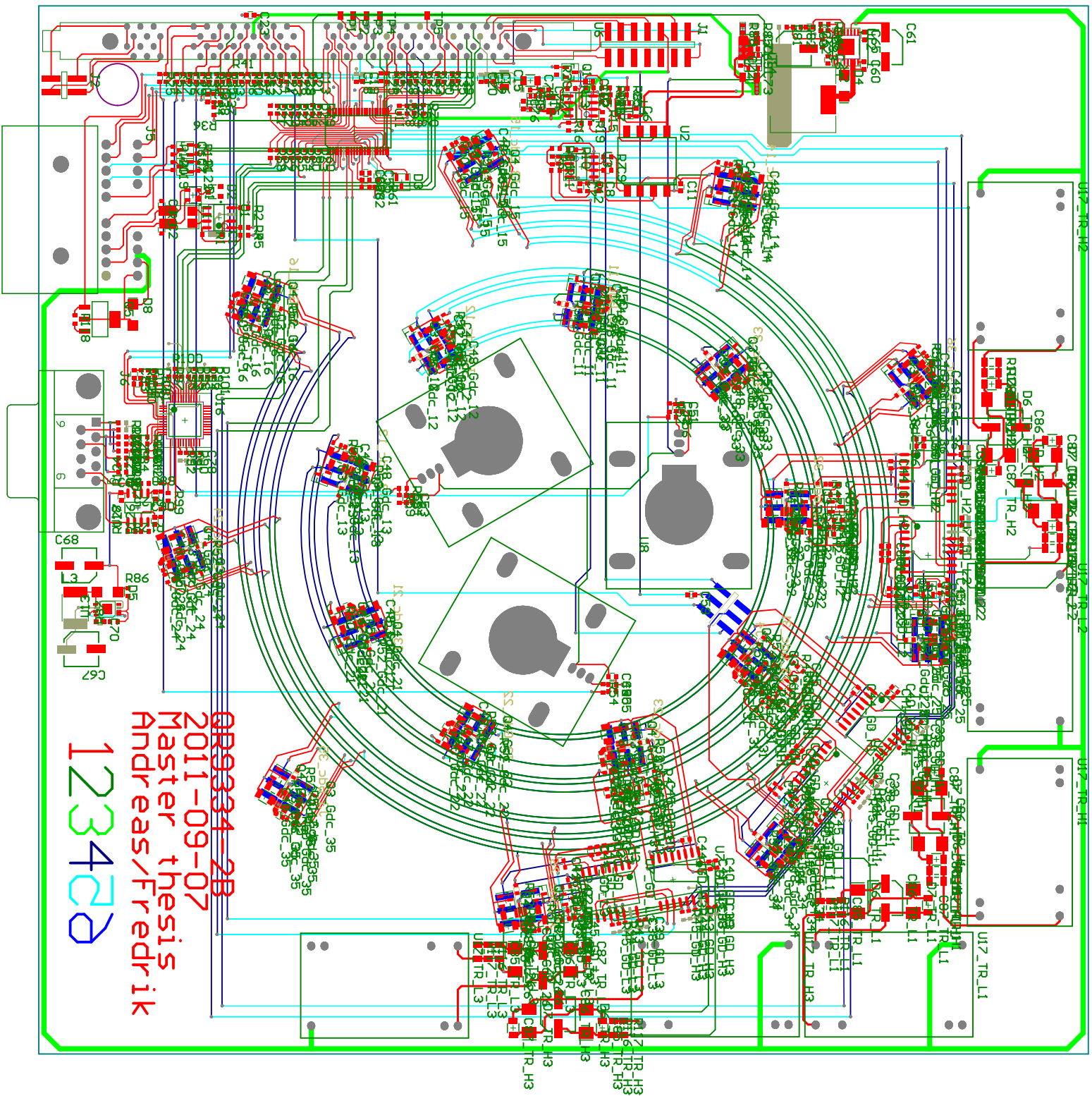
2

3

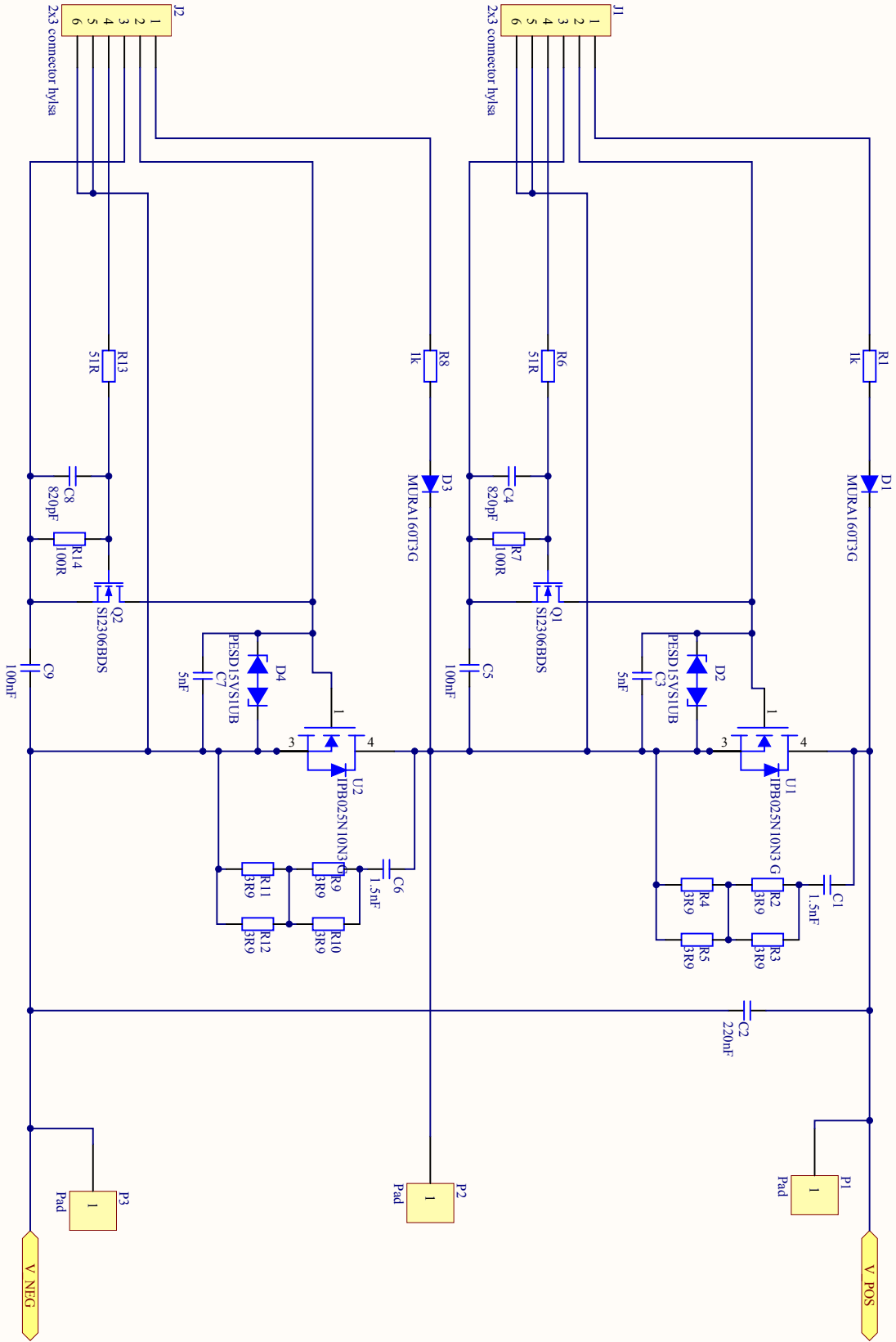
4



1	2	3	4
D	C	B	A

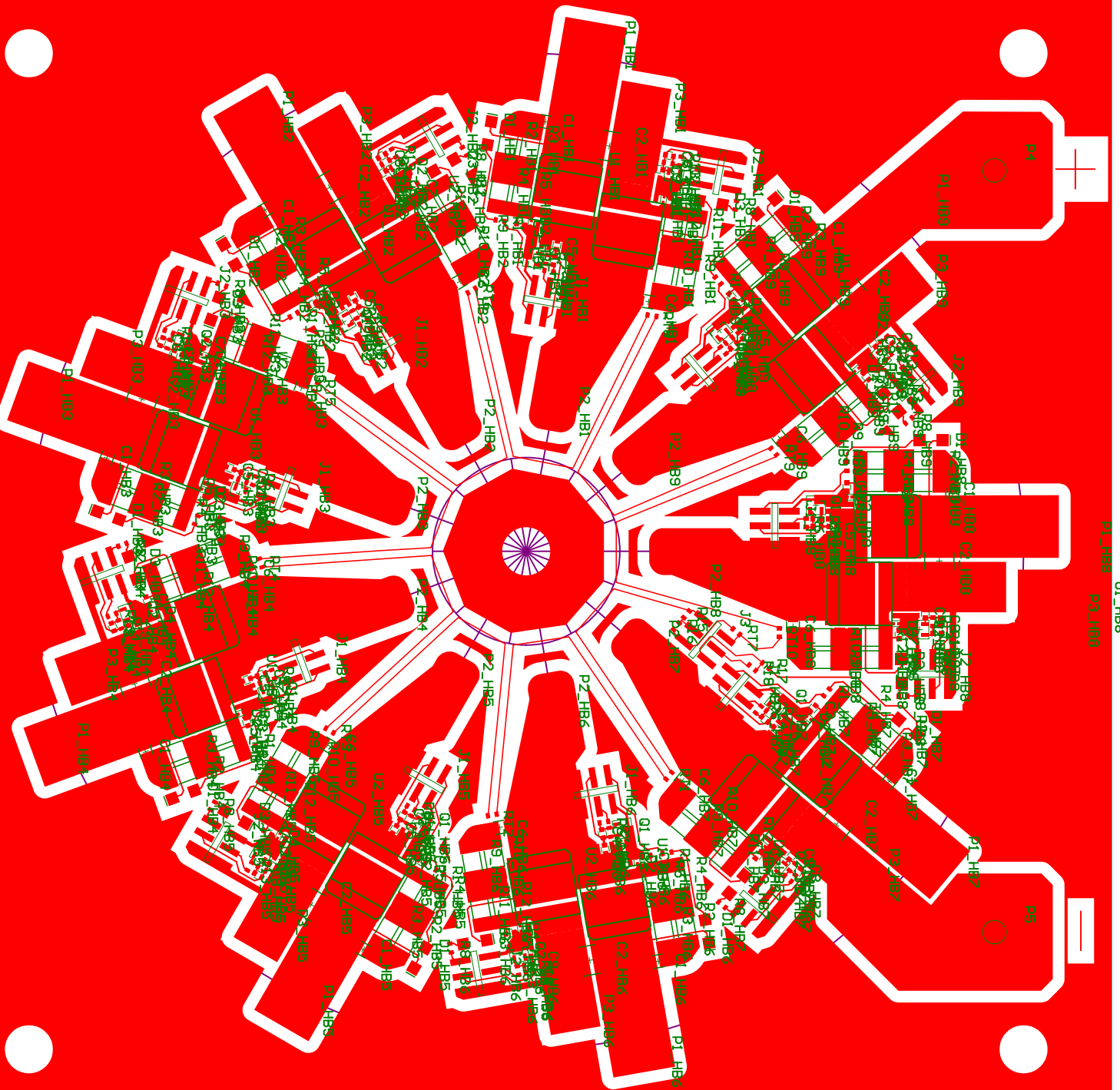


## B Power PCB schematics



Title	
Size	Number
A4	
Date:	2011-12-22
File:	P:\9334 Drivesystem Elkokant\Half bridge_Senthoobdy
Sheet of	
Revision	





P1\_HB8 U1\_HB8 U2\_HB8  
P2\_HB8

QR9334-1A

2011-09-07

Master Thesis